22/10-2-9195(2)

NIPER-533
(DE91002250)

THE THERMODYNAMIC PROPERTIES OF BENZOTHIAZOLE AND BENZOXAZOLE

Topical Report

By
W. V. Steele
R. D. Chirico
S. E. Knipmeyer
A. Nguyen

August 1991

Performed Under Cooperative Agreement No. DE-FC22-83FE60149

IIT Research Institute
National Institute for Petroleum and Energy Research
Bartlesville, Oklahoma

Bartlesville Project Office
U. S. DEPARTMENT OF ENERGY
Bartlesville, Oklahoma

NIPER-533
Distribution Category UC-125

NIPER--533

DE91 002250

THE THERMODYNAMIC PROPERTIES OF BENZOTHIAZOLE AND BENZOXAZOLE

Topical Report

By
W. V. Steele
R. D. Chirico
S. E. Knipmeyer
A. Nguyen

August 1991

Work Performed Under Coopertive Agreement No. FC22-83FE60149

Prepared for
U.S. Department of Energy
Assistant Secretary for Fossil Energy

W. D. Peters, Project Manager
Bartlesville Project Office
P. O. Box 1398
Bartlesville, OK 74005

Prepared by
IIT Research Institute
National Institute for Petroleum and Energy Research
P. O. Box 2128
Bartlesville, OK 74005

EXECUTIVE SUMMARY

Recent events have highlighted yet again the fragility of the continuity of supplies of Persian Gulf crude oil to U.S. refineries. Successive "oil crunches" have initiated discussion of ways to decrease the U.S.A.'s dependence on so valuable a resource from such a volatile area of the world. Political considerations, such as the possibility of an Americas Free Market encompassing the whole American continent (similar to the European Economic Community), could entail more extensive use of "local" oil supplies. However, much of the "local" supplies are classified as heavy petroleums; e.g., California Wilmington, Mexican Mayan, and Venezuelan Cerro Negro and Boscan. These heavy crudes each contain more heteroatoms (nitrogen in particular), more aromatics and less long-chain saturated hydrocarbons than Arabian light crude.

Even without the political considerations, the picture of crude oil refining in the U.S.A. has changed considerably in the last ten years. The world supply of petroleum crude, and light petroleum crude in particular, continues to decline. The density and, hence, complexity of refinery feedstocks have increased markedly in the last decade. The average API gravity of the crude oil run to stills in the United States dropped from approximately 34.2 in 1978 to 32.0 in 1989. That drop in API gravity has been accompanied by an equivalent increase in the amount of petroleum coke exported by the United States. When the cost of the oil imported and the price obtained for the coke are compared, it accounts for approximately **one billion dollars of the trade balance deficit per year.** The need for new technological advances in the processing of heavy petroleum is evident.

Catalytic hydrodesulfurization (HDS) is a key step in upgrading processes for conversion of light petroleum to economically viable products. Due to the increased nitrogen content of heavy petroleums relative to light crudes, and the presence of oxygen-containing compounds not prevalent in light crudes, catalytic hydrodenitrogenation (HDN) and hydrodeoxygenation (HDO) are key steps in their refining. Present HDN and HDO technology can be summarized as being HDS technology with a "much increased severity." Organic nitrogen and oxygen are commonly removed via reaction at 300 to 400 °C and 50 to 150 atm. of hydrogen. Under these severe conditions, hydrogen is consumed not only in breaking carbon-nitrogen and carbon-oxygen bonds but also in saturating aromatic components in the feed. Hydrogen consumption in excess of 1500 scf/bbl (standard cubic feet per barrel) is common in such hydrotreating situations, while the amount theoretically required for selective heteroatom removal is only about 600 scf/bbl. Hence, the saving in expensive hydrogen could be enormous if a process for denitrogenation and deoxygenation without

saturation of the aromatic rings in the feedstock could be developed. In addition the presence of both nitrogen- and oxygen-containing compounds is detrimental in present HDS technology.

This research program, funded by the Department of Energy (DOE) Office of Fossil Energy, Advanced Extraction and Process Technology (AEPT), provides accurate experimental thermochemical and thermophysical properties for "key" organic diheteroatom-containing compounds present in heavy petroleum feedstocks, and applies the experimental information to thermodynamic analyses of key HDS, HDN, and HDO reaction networks. Thermodynamic analyses, based on accurate information, provide insights for the design of cost-effective methods of heteroatom removal. The results reported here, and in a companion report to be completed, will point the way to the development of new methods of heteroatom removal from heavy petroleum.

This report details the thermodynamic properties of benzothiazole and benzoxazole. The thermodynamic properties were measured using adiabatic heat-capacity calorimetry, differential-scanning calorimetry (d.s.c.), comparative ebulliometry, inclined-piston gauge manometry, and combustion calorimetry. Critical properties were estimated from thermodynamic principles. All measured properties were combined to derive Gibbs energies of formation for a range of temperatures. With these Gibbs energies, information is accumulating for a comprehensive thermodynamic analysis of the diheteroatom-containing compound/hydrogen reaction networks. This analysis will be published within this research program.

In addition to providing the concrete base for the upcoming thermodynamic analysis, the properties reported here are particularly useful to the process-design engineer. These results, in conjunction with values for other major diheteroatom-containing compound types studied in this project, form a sound base for the development of process design correlations. Such correlations are necessary for the cost-effective, energy-efficient design of process equipment such as distillation towers, heaters, compressors, heat-exchangers, and gas-liquid reactors. A major risk associated with the lack of thermodynamic data is possible extensive derating of a plant because of undersized equipment. For example, if heat duties or vapor flow rates are underestimated during design, the installed equipment will be unable to accommodate the process streams at design flow rates resulting in less than economic operation of the plant.

ABSTRACT

Measurements leading to the calculation of the ideal-gas thermodynamic properties are reported for benzothiazole and benzoxazole. Experimental methods included combustion calorimetry, adiabatic heat-capacity calorimetry, comparative ebulliometry, inclined-piston gauge manometry, and differential-scanning calorimetry (d.s.c.). Critical property estimates are made for both compounds. Entropies, enthalpies, and Gibbs energies of formation were derived for the ideal gas for both compounds for selected temperatures between 280 K and near 650 K. The Gibbs energies of formation will be used in a subsequent report in thermodynamic calculations to study the reaction pathways for the removal of the heteroatoms by hydrogenolysis. The results obtained in this research are compared with values present in the literature. The failure of a previous adiabatic heat capacity study to see the phase transition in benzothiazole is noted. Literature vibrational frequency assignments were used to calculate ideal gas entropies in the temperature range reported here for both compounds. Resulting large deviations show the need for a revision of those assignments.

ACKNOWLEDGEMENTS

The authors gratefully acknowledge the financial support of the Office of Fossil Energy of the U.S. Department of Energy. This research was funded within the Advanced Extraction and Process Technology (AEPT) program as part of the Cooperative Agreement DE-FC22-83FE60149.

The authors acknowledge Professor E. J. "Pete" Eisenbraun and his research group at Oklahoma State University for preparation of the samples, and the assistance of I. Alex Hossenlopp in vapor-transfer of the materials prior to the calorimetric measurements.

TABLE OF CONTENTS

LIST OF TABLES

LIST OF FIGURES

GLOSSARY

This report is written with close adherence to the style adopted by The Journal of Chemical Thermodynamics. A complete description of the style can be found in the January 1991 issue of the journal. This glossary summarizes the main points with respect to the symbol usage.

Throughout this report only SI units are used in reporting thermodynamic values. All values are given in dimensionless units i.e., physical quantity = number X unit; for example $\rho/(kg \cdot m^{-3})$ rather than " ρ (kg/m^3)" or " ρ kg/m^3". Molar values, i.e., intensive functions, are denoted by the subscript "m", e.g., $C_{sat,m}$, whereas extensive functions do not have the subscript. In addition, since thermodynamic values are pressure dependent, they are reported in terms of a standard pressure p°, which in this report is 101.325 kPa (one atmosphere).

M = molar mass in $g \cdot mol^{-1}$

T = temperature in Kelvin

p = pressure in Pascals (Pa)

ρ = density in $kg \cdot m^{-3}$

$\Delta_c U^\circ_m$ = molar energy of combustion

$\Delta_c U^\circ_m/M$ = energy of combustion per gram

$\Delta_c H^\circ_m$ = molar enthalpy of combustion

$\Delta_f H^\circ_m$ = molar enthalpy of formation

$\Delta^g_l H_m$ = molar enthalpy of vaporization, hence the subscript l (for liquid) and superscript g (for gas)

$\Delta^g_l V_m$ = change in molar volume from the liquid to the real vapor

$C_{v,m}$ = molar heat capacity at constant volume

$C_{p,m}$ = molar heat capacity at constant pressure

$C_{sat,m}$ = molar heat capacity at saturated pressure

μ = chemical potential

n = number of moles of substance

V_x = volume of d.s.c. cell at a temperature T/K.

C^{II}_x = two-phase heat capacity at cell volume V_x

C^{II}_V = two-phase heat capacity at constant volume

C^{II}_V $(\rho = \rho_{sat})$ = two-phase heat capacity along the saturation line

V_l = molar volume of the liquid

T_c = critical temperature

p_c = critical pressure

ρ_c = critical density

T_r = reduced temperature = T/T_c

p_r = reduced pressure = p/p_c

ρ_r = reduced density = ρ/ρ_c

T_{tp} = triple point temperature in Kelvin

lg = $\log_{10}$

ω = acentric factor = $[-\lg (p_x/p_c) - 1]$; p_x is the vapor pressure at $T_r = 0.7$

$\Delta_0^T S_m^o$ = molar entropy at temperature T/K (relative to the entropy at T = 0 K)

$\Delta_0^T H_m^o$ = molar enthalpy at temperature T/K (relative to the crystals at 0 K)

$\Delta_{comp}S_m$ = molar entropy of compression of a gas

$\Delta_{imp}S_m$ = gas imperfection term

$T \rightarrow 0$ = Zero Kelvin

To avoid listing units in tables, entropies are reported as divided by the gas constant R, and enthalpies and Gibbs energies are generally reported divided by the product of the gas constant and temperature, R·T. Units of time are s (seconds) or h (hours).

1. INTRODUCTION

This report details thermochemical and thermophysical property measurements on the diheteroatom-containing aromatic compounds benzothiazole and benzoxazole. This research is funded by the Department of Energy (DOE) Office of Fossil Energy, within the Advanced Extraction and Process Technology (AEPT) program.

It has been well documented,[e.g., 1-4] that the hydrodesulfurization (HDS) of petroleum crude feedstocks is inhibited by the presence of oxygen- and nitrogen-containing compounds. Similarly, the hydrodeoxygenation (HDO) of coal liquids is inhibited by the presence of nitrogen-containing compounds. In these instances, it is evident that the effect of competitive adsorption on the catalyst sites is the dominant factor. Studies on compounds where either sulfur or oxygen is present with nitrogen within the same molecule are rare. Such studies would give insights into the processes occurring on the catalyst surface during either HDS or HDO.

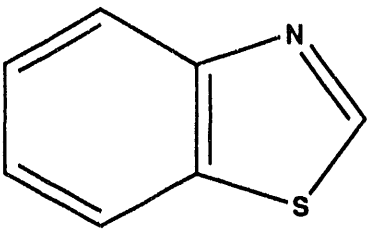

BENZOTHIAZOLE

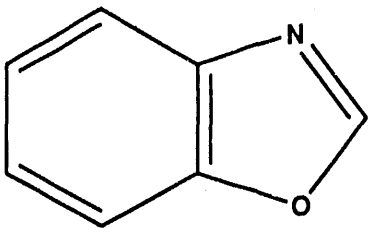

BENZOXAZOLE

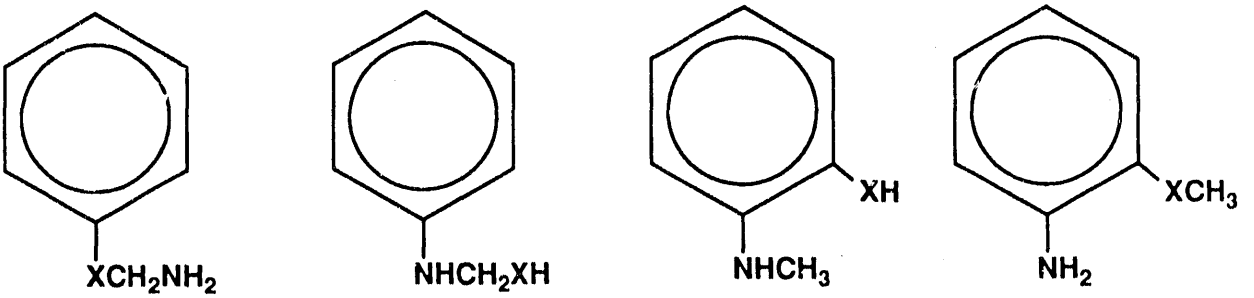

PRODUCTS OF HYDROGENOLYSIS
X = S OR O

In the HDS or HDO of aromatic 5-membered ring systems, saturation of the double bond in the heterocyclic ring is required prior to ring cleavage.[5,6] In the subsequent hydrogenolysis (ring opening) of benzothiazole or benzoxazole a range of

substituted benzenes can be formed depending on where the five-membered ring opens, as shown above.

Konuma et al[7,8] studied the HDS of benzothiazole on a Mo(VI) sulfide catalyst under 40 atmospheres hydrogen pressure in the temperature range 240 °C to 280 °C. At the lower temperature they noted 38 per cent conversion with 28 percent anilines selectivity. At 280 °C, conversion rose to greater than 99 per cent with greater than 90 per cent anilines selectivity. In contrast, the same group,[9] operating with the same catalyst, obtained only 7 per cent conversion for benzoxazole at 280 °C and 54 per cent at 320 °C with almost complete selectivity to ortho-aminophenol in both cases.

The results presented in this report form the first step in a thermodynamic analysis of the HDS of benzothiazole, the HDO of benzoxazole, and the HDN (hydro-denitrogenation) of both compounds. The results of the thermodynamic analysis will delineate the presence of any reaction steps occurring under thermodynamic control within the reaction schemes. Hence, the analysis will show if any restricted pathways exist within the reaction schemes. The thermodynamic analysis will be the subject of a future topical report from this group. While neither benzothiazole or benzoxazole have been listed as important constituents of heavy petroleum, oil shale, or the products of the liquefaction of coal, both have been found in the products of the oxidative degradation of Gudao asphaltene.[10]

2. EXPERIMENTAL

MATERIALS

A commercial sample of benzoxazole was purified by vacuum distillation at 325 K (0.08 kPa), and was sealed in glass under vacuum. A commercial sample of benzothiazole was purified as follows. A freshly distilled sample was reacted with oxalic acid in a (water+propan-2-ol) mixture. The resulting oxalate was recrystallized twice from a mixture of (water+propan-2-ol) in equal proportions by mass. The oxalate was cleaved by reaction with base (KOH + water) in the proportion 3 g KOH to 4 g water. The liberated benzothiazole was extracted with diethyl ether. The extract was washed with water, dried (Na_2CO_3), filtered, concentrated under vacuum, doubly distilled at 320 K (0.06 kPa), and sealed under vacuum in glass ampoules. All subsequent sample transfers were done under vacuum or an inert (nitrogen or helium) atmosphere.

The mole-fraction impurity for each sample was estimated to be less than 0.0001 using g.l.c. The high purities of the samples were corroborated in the fractional-melting studies completed as part of the adiabatic heat-capacity studies, and

the small differences between the boiling and condensation temperatures observed in the ebulliometric vapor-pressure studies discussed later.

The water used as a reference material in the ebulliometric vapor-pressure measurements was deionized and distilled from potassium permanganate. The decane used as a reference material for the ebulliometric measurements was purified by urea complexation, two recrystallizations of the complex, decomposition of the complex with water, extraction with ether, drying with $MgSO_4$, and distillation at 337 K and 1 kPa pressure.

PHYSICAL CONSTANTS AND STANDARDS

Molar values are reported in terms of M = 135.183 $g \cdot mol^{-1}$ and 119.123 $g \cdot mol^{-1}$ for benzothiazole and benzoxazole, respectively, based on the relative atomic masses of 1981[11]† and the gas constant R = 8.31451 $J \cdot K^{-1} \cdot mol^{-1}$ adopted by CODATA.[12] The platinum resistance thermometers used in these measurements were calibrated by comparison with standard thermometers whose constants were determined at the National Institute of Standards and Technology (NIST), formerly the National Bureau of Standards (NBS). All temperatures reported are in terms of the IPTS-68.[13] The platinum resistance thermometer used in the adiabatic heat-capacity studies was calibrated below 13.81 K with the method of McCrackin and Chang.[14] Measurements of mass, time, electrical resistance, and potential difference were made in terms of standards traceable to calibrations at NIST

APPARATUS AND PROCEDURES

Combustion Calorimetry. The experimental procedures used in the combustion calorimetry of organic compounds containing nitrogen, sulfur, and oxygen at the National Institute for Petroleum and Energy Research have been described.[15-18] A rotating-bomb calorimeter (laboratory designation BMR II)[19] and platinum-lined bomb (laboratory designation Pt-3b)[20] with an internal volume of 0.3934 dm^3 were used. In the measurements on benzothiazole the bomb rotation mechanism started 100 s after ignition of the sample and remained on to the end of each experiment. In the benzoxazole combustions the bomb was not rotated.

Temperatures were measured by quartz-crystal thermometry.[21,22] A computer was used to control the combustion experiments and record the results. The

---

† The 1981 relative atomic masses were used because the CODATA Recommended Key Values for Thermodynamics (reference 37) are based on them.

quartz-crystal thermometer was calibrated by comparison with a platinum resistance thermometer. Counts of the crystal oscillation were taken over periods of 100 s throughout the experiments. Integration of the time-temperature curve is inherent in the quartz-crystal thermometer readings.[23]

Ebulliometric Vapor-Pressure Measurements. The essential features of the ebulliometric equipment and procedures are described in the literature.[24,25] The ebulliometers were used to reflux the substance under study with a standard of known vapor pressure under a common helium atmosphere. The boiling and condensation temperatures of the two substances were determined, and the vapor pressure was derived with the condensation temperature of the standard.[26]

The precision in the temperature measurements for the ebulliometric vapor-pressure studies was 0.001 K. The precision in pressure is adequately described by:

$$\sigma(p) = (0.001\ \mathrm{K})\{(dp_{ref}/dT)^2 + (dp_x/dT)^2\}^{1/2}\ , \qquad (1)$$

where p_{ref} is the vapor pressure of the reference substance and p_x is the vapor pressure of the sample under study. Values of dp_{ref}/dT for the reference substances were calculated from fits of the Antoine equation[27] to vapor pressures of the reference materials (decane and water) reported in reference 26.

Inclined-Piston Vapor-Pressure Measurements. The equipment for the inclined-piston vapor-pressure measurements has been described by Douslin and McCullough,[28] and Douslin and Osborn.[29] Recent revisions to the equipment and procedures have been reported.[30] Uncertainties in the pressures determined with the inclined-piston apparatus, on the basis of estimated precision of measuring the mass, area, and angle of inclination of the piston, are adequately described by the expression:

$$\sigma(p)/\mathrm{Pa} = 1.5\cdot10^{-4}(p/\mathrm{Pa}) + 0.200\ . \qquad (2)$$

The uncertainties in the temperatures are 0.001 K.

Adiabatic Heat-Capacity Calorimetry. Adiabatic heat-capacity and enthalpy measurements were made with a calorimetric system described previously.[30] The calorimeter characteristics and scaling conditions are given in table 1.¶ Energy

¶ All tables are given at the end of this report.

measurement procedures were the same as those described for studies on quinoline.[30] Thermometer resistances were measured with self-balancing, alternating-current resistance bridges (H. Tinsley & Co. Ltd.; Models 5840C and 5840D). Energies were measured to a precision of 0.01 per cent, and temperatures were measured to a precision of 0.0001 K. The energy increments to the filled platinum calorimeters were corrected for enthalpy changes in the empty calorimeters, for the helium exchange gas, and for vaporization of the samples. The maximum correction to the measured energies for the helium exchange gas was 0.1 per cent near 5 K. The sizes of the other two corrections are indicated in table 1.

Differential-Scanning Calorimetry (d.s.c.). Differential-scanning calorimetric measurements were made with a Perkin-Elmer DSC-2. Experimental methods were described previously.[31-33]

3. RESULTS

COMBUSTION CALORIMETRY

NBS benzoic acid (sample 39i) was used for calibration of the combustion bomb calorimeter; its specific energy of combustion is $-(26434.0\pm3.0)$ $J\cdot g^{-1}$ under certificate conditions. Conversion to standard states[34] gives $-(26413.7\pm3.0)$ $J\cdot g^{-1}$ for $\Delta_c U^\circ_m/M$, the specific energy of the idealized combustion reaction. Calibration experiments without bomb rotation were interspersed with the benzoxazole measurements. Nitrogen oxides were not formed in the calibration experiments due to the high purity of the oxygen used and preliminary bomb flushing. The energy equivalent of the calorimeter obtained for the calibration series, ε(calor), was (16773.0 ± 0.4) $J\cdot K^{-1}$ (mean and standard deviation of the mean). Six calibration experiments with rotation of the bomb were interspersed with the benzothiazole combustion measurements. In that calibration series $10.0\cdot10^{-3}$ dm^3 of water was added to the bomb to mimic the sulfur-compound experiments. The energy equivalent of the calorimeter obtained in that calibration series was ε(calor) = (16772.0 ± 0.4) $J\cdot K^{-1}$ (mean and standard deviation of the mean).

For each experiment with the sulfur-containing compound, one atmosphere of air was left in the bomb, $10.0\cdot10^{-3}$ dm^3 of water was added, and it was subsequently charged with pure oxygen to a total pressure of 3.04 MPa. (The atmosphere of air left in the bomb contained sufficient nitrogen, which -- in the presence of the platinum crucible and lining -- acted as a catalyst for the conversion of any SO_2 formed to SO_3, and hence, dilute sulfuric acid. During the catalysis reaction some of the available

nitrogen was converted to NO_2, and hence, formed nitric acid upon dissolving in the water present.) For each benzoxazole experiment $1.0 \cdot 10^{-3}$ dm^3 of water was added, and the bomb was flushed and subsequently charged with pure oxygen to a total pressure of 3.04 MPa. Flexible borosilicate glass ampoules[15] were used to confine both samples. Judicious choice of sample and auxiliary masses allowed the temperature rise in each combustion series and its corresponding calibration series to be the same within 0.1 per cent. All experiments were completed within 0.01 K of 298.15 K.

The auxiliary oil (laboratory designation TKL66) had the empirical formula $CH_{1.913}$, and $\Delta_c U^o_m = -(46042.5 \pm 1.8)$ $J \cdot g^{-1}$ (mean and standard deviation). For the cotton fuse, empirical formula $CH_{1.774}O_{0.887}$, $\Delta_c U^o_m = -16945$ $J \cdot g^{-1}$.

Nitric acid, nitrous acid, and total acids were determined quantitatively in the combustions of benzothiazole.[35] The amount of sulfuric acid was obtained by difference and agreed, within experimental uncertainties, with that calculated from the stoichiometry.

Nitric acid formed during the benzoxazole combustions was determined by titration with standard sodium hydroxide.[35] Carbon dioxide was recovered from the combustion products of each benzoxazole experiment and its calibration series. (No CO_2 recoveries were made for the benzothiazole series due to the presence of the relatively large volume of water.) Anhydrous lithium hydroxide was used as absorbent.[16] Carbon dioxide percentage recoveries were 99.990±0.005 (mean and standard deviation of the mean) for the calibrations and 99.969±0.013 for the corresponding benzoxazole combustions. In all experiments the combustion products were checked for unburned carbon and other products of incomplete combustion, but none were detected.

Auxiliary information, necessary for reducing apparent masses to masses, converting the energy of the actual bomb process to that of the isothermal process, and reducing to standard states,[34] included a density at 298.15 K of 1237 $kg \cdot m^{-3}$ and an estimated value of $8 \cdot 10^{-7}$ $m^3 \cdot K^{-1}$ for $(\partial V_m/\partial T)_p$ for benzothiazole. For benzoxazole values of 1245 $kg \cdot m^{-3}$ and $4 \cdot 10^{-7}$ $m^3 \cdot K^{-1}$ were used for the density and $(\partial V_m/\partial T)_p$ respectively. The densities were obtained by weighing filled ampoules of known volume. The molar heat capacities at 298.15 K for benzothiazole and benzoxazole used in the corrections to standard states are given as part of the heat-capacity study results later in this report.

Typical combustion experiments for benzothiazole and benzoxazole are summarized in table 2. It is impractical to list summaries for each combustion, but values of $\Delta_c U^o_m/M$ for all the experiments are reported in table 3. For benzoxazole values of $\Delta_c U^o_m/M$ in table 3 refer to the reaction:

$$C_7H_5NO(cr) + 7.75\ O_2(g) = 7\ CO_2(g) + 2.5\ H_2O(l) + 0.5\ N_2(g). \quad (3a)$$

For benzothiazole values of $\Delta_c U^o_m/M$ in table 3 refer to the reaction:

$$C_7H_5NS(l) + 9.75\ O_2(g) + 113.5\ H_2O(l) = 7\ CO_2(g) + 0.5\ N_2(g) + H_2SO_4 \cdot 115H_2O(l). \quad (3b)$$

Table 3 also gives derived values of the standard molar energy of combustion $\Delta_c U^o_m$, the standard molar enthalpy of combustion $\Delta_c H^o_m$, and the standard molar enthalpy of formation $\Delta_f H^o_m$, for benzoxazole and benzothiazole. Values of $\Delta_c U^o_m$ and $\Delta_c H^o_m$ refer to reaction (**3a**) or (**3b**). The values of $\Delta_f H^o_m$ refer to reaction (**4**) for benzoxazole and reactions (**4a**) and (**4b**) for benzothiazole:

$$7\ C(cr, graphite) + 2.5\ H_2(g) + 0.5\ N_2(g) + 0.5\ O_2(g) = C_7H_5NO(cr), \quad (4)$$

$$7\ C(cr, graphite) + 2.5\ H_2(g) + 0.5\ N_2(g) + S\ (cr, rhombic) = C_7H_5NS(l), \quad (4a)$$

$$7\ C(cr, graphite) + 2.5\ H_2(g) + 0.5\ N_2(g) + 0.5\ S_2(g) = C_7H_5NS(l). \quad (4b)$$

(Historically, enthalpies of formation for sulfur-containing compounds have been published with two different reference states for sulfur, $S_2(g)$ and S (cr, rhombic). Values relative to each reference state are given in table 3.) Uncertainties given in table 3 are the "uncertainty interval" defined in reference 36. The enthalpies of formation of $CO_2(g)$, $H_2O(l)$, $H_2SO_4 \cdot 115H_2O$, and $S_2(g)$ were taken to be $-(393.51 \pm 0.13)$, $-(285.830 \pm 0.042)$, $-(887.81 \pm 0.40)$, (128.49 ± 0.30) kJ·mol^{-1}, respectively, as assigned by CODATA.[37]

VAPOR-PRESSURE MEASUREMENTS

Vapor pressures for benzothiazole and benzoxazole are reported in table 4. Following previous practice,[25] the results obtained in the ebulliometric measurements were adjusted to common pressures. The common pressures, the condensation temperatures, and the difference between condensation and boiling temperatures ΔT for the samples are reported. For both benzothiazole and benzoxazole the small differences between the boiling and condensation temperatures (column 6 table 4) indicated correct operation of the equipment and the high purity of the samples. At the highest temperatures measured for benzothiazole, the increase in ΔT relative to that for the previous temperature is indicative of some sample decomposition. Measurements on benzothiazole by d.s.c. described later showed rapid sample decomposition for temperatures above 600 K.

Cox Equation Fits to Vapor Pressures. The Cox equation[38] in the form:

$$\ln(p/p_{ref}) = \{1 - (T_{ref}/T)\}\exp\{A + B(T/K) + C(T/K)^2\}\,, \qquad (5)$$

was fitted to the experimental vapor pressures with fixed p_{ref} and T_{ref} values listed in table 5. The values of p_{ref} and T_{ref} used for benzoxazole were the p_c and T_c obtained in the simultaneous fittings of the vapor pressures and the d.s.c. two-phase heat capacities discussed later in this report. For benzothiazole, the T_{ref} value is an estimate of T_c derived from the group-contribution parameters of Joback[39,40] and Somayajulu,[41] with the normal-boiling temperature determined in this research. The value for p_{ref} was allowed to vary in the fit. Because the uncertainties in p_{ref} and T_{ref} for benzothiazole are difficult to assess, extrapolations of the benzothiazole vapor-pressure results were limited to 50 K.

The vapor-pressure fitting procedure has been described.[26,30] Parameters derived from the fits are given in table 6. Details of the Cox equation fits are given in table 4.

Derived Enthalpies of Vaporization. Enthalpies of vaporization $\Delta_l^g H_m$ were derived from the Cox equation fits by means of the Clapeyron equation:

$$dp/dT = \Delta_l^g H_m / (T\,\Delta_l^g V_m)\,. \qquad (6)$$

$\Delta_l^g V_m$ is the increase in molar volume from the liquid to the real vapor. The Cox equation fits were employed to derive dp/dT. Estimates of liquid-phase volumes were made with the extended corresponding-states equation of Riedel,[42] as formulated by Hales and Townsend:[43]

$$(\rho/\rho_c) = 1.0 + 0.85\{1.0 - (T/T_c)\} + (1.692 + 0.986\omega)\{1.0 - (T/T_c)\}^{1/3}\,, \qquad (7)$$

with $\rho_c = 380\ \mathrm{kg\cdot m^{-3}}$, $T_c = 771$ K, and an acentric factor $\omega = 0.355$ for benzothiazole, and $\rho_c = 349\ \mathrm{kg\cdot m^{-3}}$, $T_c = 695$ K, and an acentric factor $\omega = 0.362$ for benzoxazole. The uncertainty in the liquid-phase volumes was estimated to be 3 per cent. [The acentric factor is defined as $\{-\lg(p/p_c) - 1\}$, where p is the vapor pressure at $T_r = 0.7$ and p_c is the critical pressure.] The Cox-equation coefficients given in table 5 were used to calculate p. The critical density for benzothiazole was estimated with equation (7) and a liquid-phase density value {$(1250\pm30)\ \mathrm{kg\cdot m^{-3}}$ at 285.7 K} determined during filling of the calorimeter for heat-capacity measurements by adiabatic

calorimetry. Similarly, a critical density for benzoxazole was estimated with equation (7) and a liquid-phase density value of (1100±30) $kg \cdot m^{-3}$ at 310.2 K.

Vapor-phase volumes were calculated with the virial equation of state truncated at the third virial coefficient. Second virial coefficients were estimated with the corresponding-states equation of Pitzer and Curl,[44] and third virial coefficients were estimated with the corresponding-states method of Orbey and Vera.[45] This formulation for third virial coefficients was applied successfully in analyses of the thermodynamic properties of benzene, toluene, and decane.[46] Third virial coefficients are required for accurate calculation of the gas volume for pressures greater than 1 bar. Uncertainties in the virial coefficients are assumed to be 10 per cent. Derived enthalpies of vaporization are reported in table 6. For p>1 bar the uncertainties in the virial coefficients are the dominant contributions to the uncertainties in the derived enthalpies of vaporization.

ADIABATIC HEAT-CAPACITY CALORIMETRY

Crystallization and Melting Studies. Crystallizations of benzothiazole and benzoxazole were initiated by slowly cooling (approximately 2 $mK \cdot s^{-1}$) the liquid samples roughly 10 K below their respective triple-point temperatures. Complete crystallization was ensured by maintaining the samples under adiabatic conditions in the partially melted state (10 to 20 per cent liquid) for approximately 24 h. For benzoxazole, no spontaneous warming, which would indicate incomplete crystallization, was observed in this time period. The benzothiazole sample warmed for approximately 8 h. The samples were cooled at an effective rate of 2 $mK \cdot s^{-1}$ to crystallize the remaining liquid. Finally, the samples were thermally cycled from <100 K to within 2 K of their triple-point temperatures, where they were held for a minimum of 8 h to provide further tempering. All of the solid-phase measurements were performed upon crystals pre-treated in this manner.

The triple-point temperatures T_{tp} and sample purities were determined by measurement of the equilibrium melting temperatures T(F) as a function of fraction F of the sample in the liquid state.[47] Equilibrium melting temperatures were determined by measuring temperatures at approximately 300-s intervals for 0.8 to 1.2 h after an energy input and extrapolating to infinite time by assuming an exponential decay toward the equilibrium value. The observed temperatures at 1 h after an energy input were invariably within 3 mK of the calculated equilibrium temperatures for F values listed in table 8. The results did not indicate the presence of solid-soluble impurities, and

published procedures[48] were used to derive the mole fractions of impurities and triple-point temperatures. The results are summarized in table 7.

Phase Transformations and Enthalpy Measurements. Experimental molar enthalpy results are summarized in table 8. The table includes both phase-transition enthalpies and single-phase measurements, which serve as checks on the integration of the heat-capacity results. Corrections for pre-melting caused by impurities were made in these evaluations. Results with the same series number in tables 8 and 9 were taken without interruption of adiabatic conditions.

Excellent reproducibility (within ±0.01 per cent) was obtained in the enthalpy-of-fusion results for each compound. This implies that cr(I) phases were formed reproducibly by means of the tempering methods described above. Both compounds showed a single solid-phase transition near 245 K with little associated enthalpy.

Prior to measurements of the transition enthalpy for benzothiazole, the sample was annealed between 239 K and 243 K for 2 d, 3 d, 11 d, and 0.8 d for series 8, 9, 13, and 14, respectively. Because of the small difference between the result obtained after 11 d of annealing (series 13) and 3 d of annealing (series 9), the series 13 results were used to calculate the enthalpy across the transition region for all further calculations. The difference between the series 14 and series 13 results provides an estimate of the minimum total enthalpy associated with the conversion from cr(I) to cr(II).

Prior to measurements of the transition enthalpy for benzoxazole, the sample was annealed between 240 K and 243 K for 0.2 d, 10 d, and 15 d for series 3, 4, and 8, respectively. No warming was observed after 10 d during sample annealing prior to series 8. This is consistent with the agreement between the series 4 and series 8 results. The small difference is not significant. The series 3 result shows the effect of the failure to anneal the low-temperature form.

Heat Capacity Measurements. The experimental molar heat capacities under vapor saturation pressure $C_{sat,m}$ determined by adiabatic calorimetry are listed in table 9. Values in table 9 were corrected for effects of sample vaporization into the gas space of the calorimeter. The temperature increments were small enough to obviate the need for corrections for non-linear variation of $C_{sat,m}$ with temperature except near phase-transition temperatures. The precision of the heat-capacity measurements ranged from approximately 5 per cent at 5 K, to 2 per cent at 11 K, 0.2 per cent near 20 K, and improved gradually to less than 0.1 per cent above 100 K, except in the solid phase

near the triple-point and solid-phase transition temperature where equilibration times were long. The heat capacities in table 9 have not been corrected for pre-melting, but from the temperature increments provided an independent calculation can be made. Curves of heat capacity against temperature are shown in figures 1 and 2. Results above 450 K were determined by d.s.c. as described later.

For heat-capacity measurements in the liquid phase and in cr(II) below 238 K, equilibrium was reached in less than 1 h for both compounds. For benzothiazole above 238 K, equilibration times increased to 3 h at 240 K, approximately 40 h between 243 K and 248 K, and 12 h for all measurements above 255 K in phase cr(I). Similarly for benzoxazole above 238 K, equilibration times increased to 3 h at 241 K, and roughly 36 h for all measurements above 255 K in phase cr(I). No attempt was made to equilibrate the benzoxazole sample in the 241 K to 251 K range.

Details of the heat-capacity and enthalpy measurements in the cr(II)-to-cr(I) transition regions are shown in figures 3 and 4. The heat-capacity curves are not defined uniquely in the immediate vicinity of the transitions from cr(II) to cr(I), as represented by the dashed lines in the figures. The heat-capacity curves shown were used to calculate the enthalpy-of-transition values listed in table 8. (Heat-capacity values sufficient to define these curves are included in table 10.) Uncertainty in the transition temperatures is approximately ±2 K. The uncertainty in the shape of the heat-capacity curve has no effect on the derived condensed-phase enthalpies above 250 K, and an insignificant effect on the derived entropies. For the purpose of the entropy calculations, all of the excess enthalpy at T_{trs} listed in table 8 was assumed to occur at T_{trs}. Extrapolation of the heat-capacity results to $T \rightarrow 0$ was made by extrapolation of a plot of $C_{sat,m}/T$ against T^2 for results below 10 K.

DIFFERENTIAL SCANNING CALORIMETRY

Theoretical Background. The theoretical background for the determination of heat capacities for the liquid phase at vapor-saturation pressure $C_{sat,m}$ with results obtained with a d.s.c. has been described.[31,32,49] If two phases are present and the liquid is a pure substance, then the vapor pressure p and the chemical potential μ are independent of the amount of substance n and the cell volume V_x, and are equal to p_{sat} and μ_{sat}. The two-phase heat capacities at cell volume V_x, $C^{II}_{x,m}$, can be expressed in terms of the temperature derivatives of these quantities:

$$n C^{II}_{x,m}/T = -n(\partial^2\mu/\partial T^2)_{sat} + V_x (\partial^2 p/\partial T^2)_{sat} + (\partial V_x/\partial T)_x(\partial p/\partial T)_{sat}. \quad (8)$$

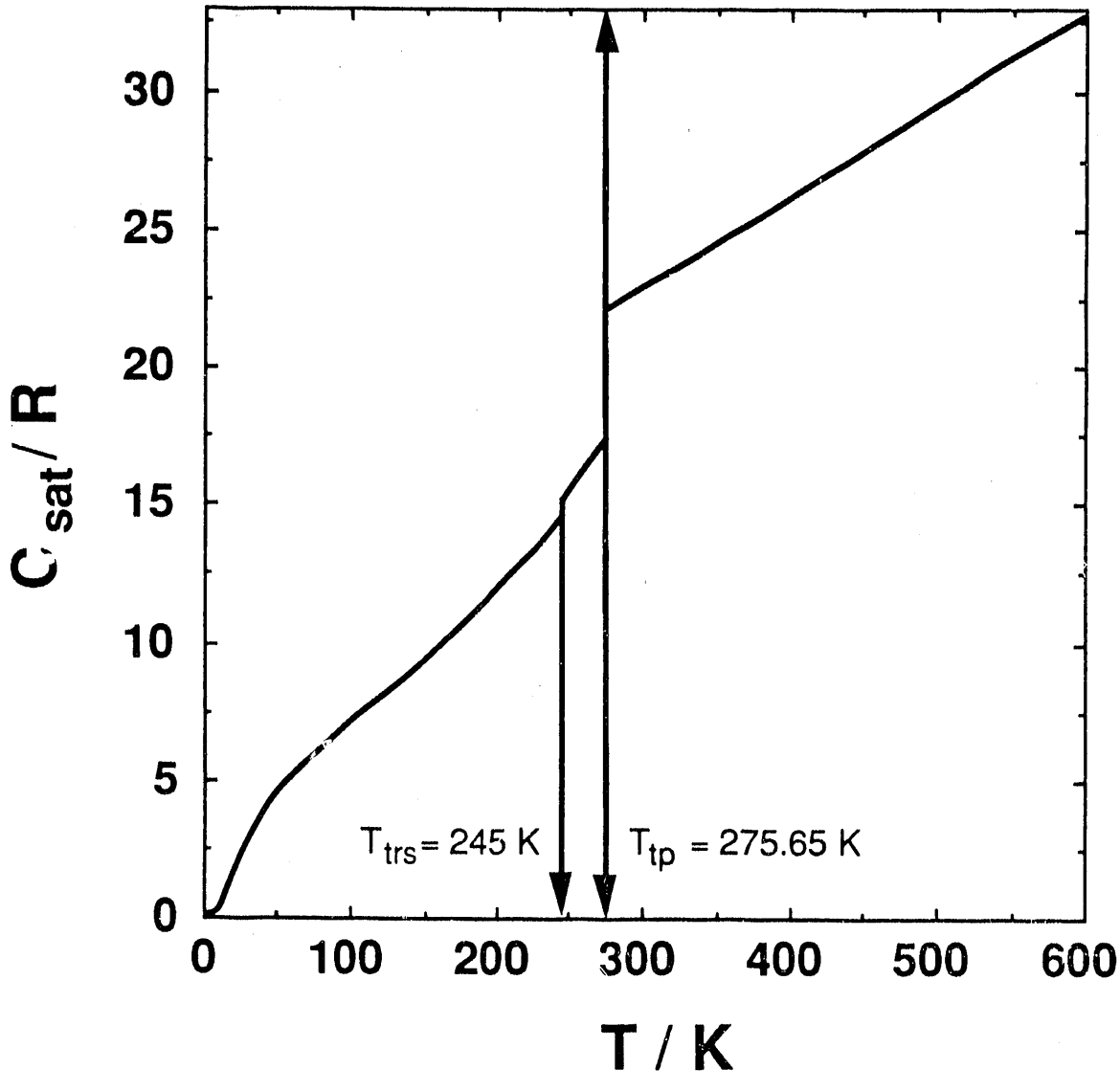

FIGURE 1. Curve of heat capacity against temperature for benzothiazole. The vertical lines indicate phase-transition temperatures.

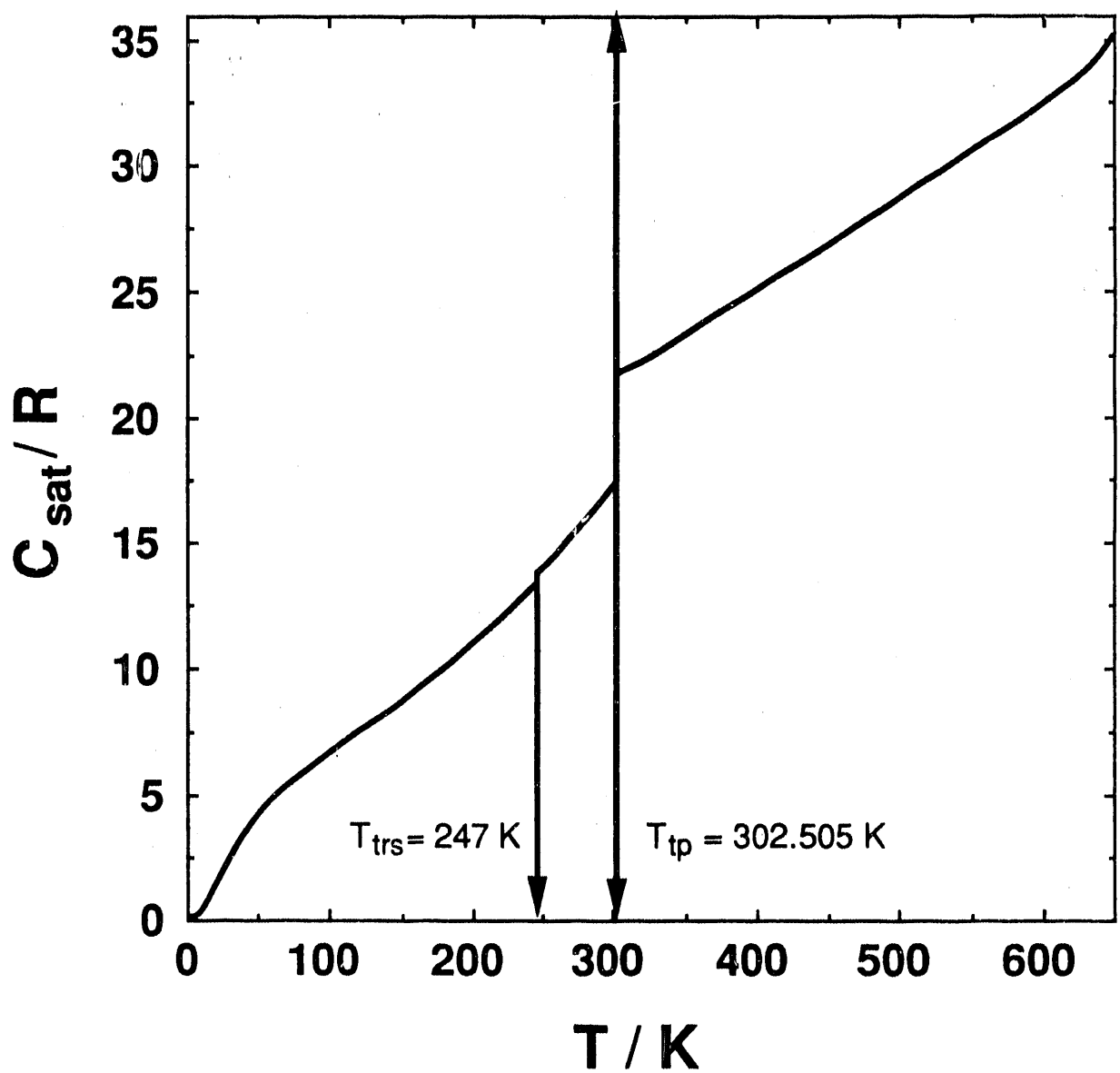

FIGURE 2. Curve of heat capacity against temperature for benzoxazole. The vertical lines indicate phase-transition temperatures.

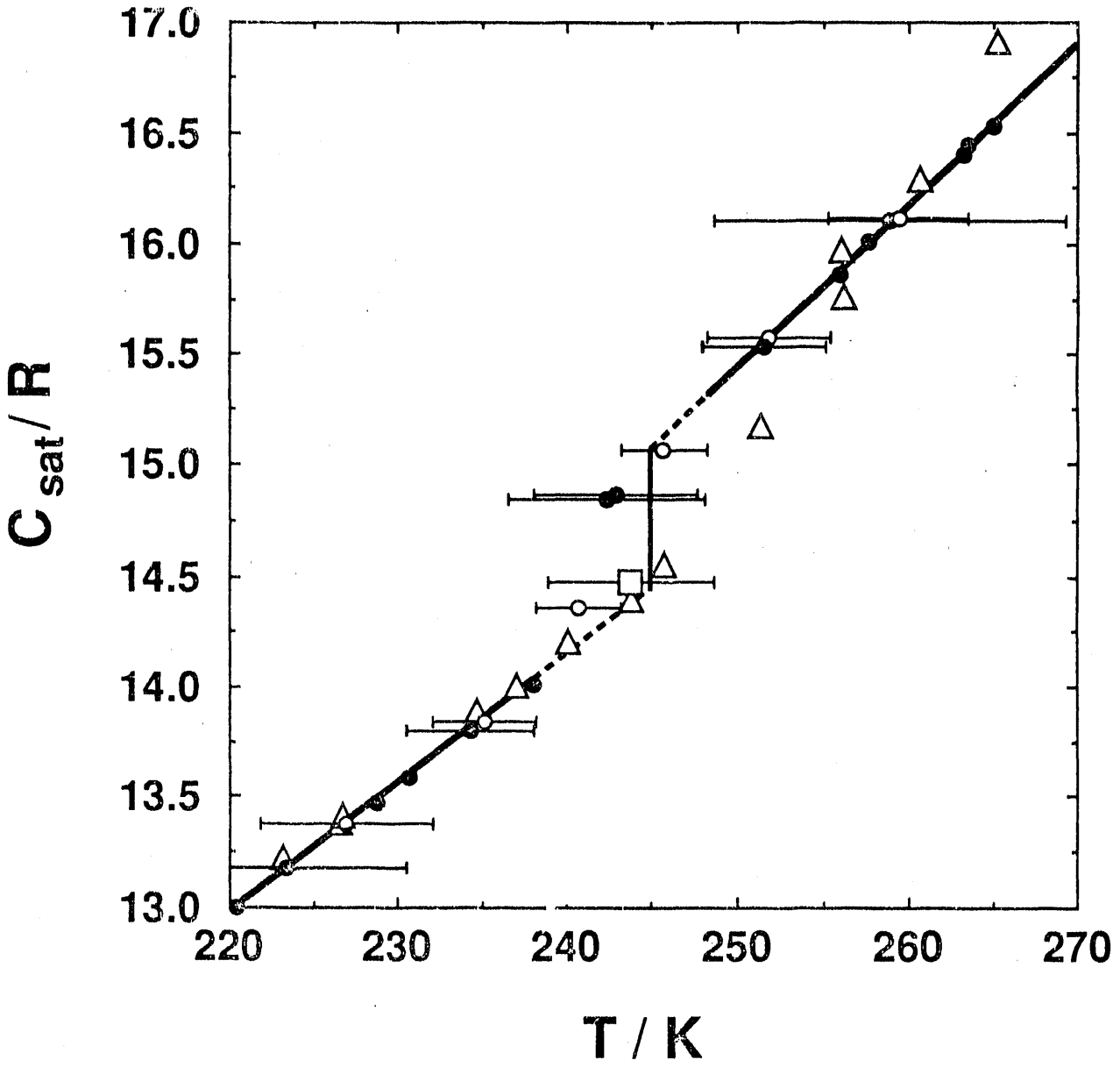

FIGURE 3. Average heat capacities in the cr(II)-to-cr(I) transition region for benzothiazole. ●, Series 3, 4, 5, 6, 7, 9, and 13; □, series 14; ○, series 8; △, Goursot and Westrum.[57] Dashed lines represent the region in which the heat-capacity curve is not defined uniquely. The heat-capacity curve is defined in the text. The horizontal bars span the temperature increments associated with the average heat-capacity values. For clarity these are shown only for series which span T_{trs}. No temperature increments were reported by Goursot and Westrum.

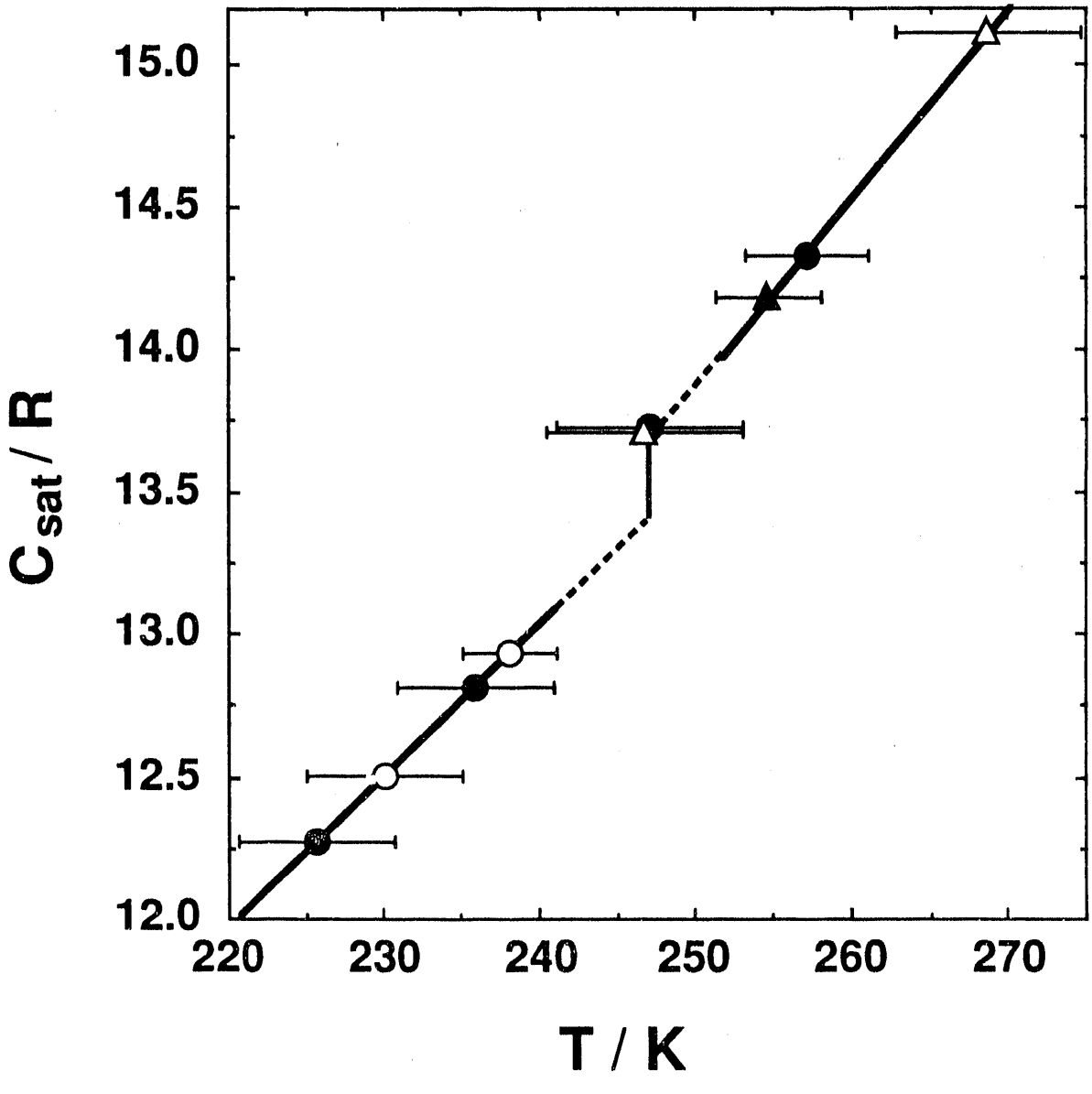

FIGURE 4. Average heat capacities in the cr(II)-to-cr(I) transition region for benzoxazole. ▲, Series 3; ●, series 4; ○, series 5; △, series 8. Dashed lines represent the region in which the heat-capacity curve is not defined uniquely. The heat-capacity curve is described in the text. The horizontal bars span the temperature increments associated with the average heat-capacity values.

The third term on the right-hand side of equation (**8**) includes the thermal expansion of the cell. In this research the thermal expansion of the cells was expressed as:

$$V_X(T) \,/\, V_X(298.15\ K) = 1 + ay + by^2, \qquad (9)$$

where, $y = (T - 298.15)$ K, $a = 3.216 \times 10^{-5}\ K^{-1}$, and $b = 5.4 \times 10^{-8}\ K^{-2}$.

Values of $(\partial p/\partial T)_{sat}$ can be calculated based on the vapor pressures measured in this research. Therefore, with a minimum of two different filling levels of the cell, $(\partial^2 p/\partial T^2)_{sat}$ and $(\partial^2 \mu/\partial T^2)_{sat}$ can be determined. In this research three fillings were used. To obtain the saturation heat capacity $C_{sat,m}$ at vapor pressures greater than 0.1 MPa, the limit where the cell is full of liquid is required; i.e., $(n/V_x) = \{1/V_m(l)\}$ where $V_m(l)$ is the molar volume of the liquid:

$$\lim_{(n/V_x) \to \{1/V_m(l)\}} (n\, C^{II}_{v,m}/T) = V_m(l)(\partial^2 p/\partial T^2)_{sat} - n(\partial^2 \mu/\partial T^2)_{sat}. \qquad (10)$$

$C_{sat,m}$ is obtained from the expression:

$$C_{sat,m} = (1/n)\cdot\left\{ \lim_{(n/V_x) \to \{1/V_m(l)\}} (n\, C^{II}_{v,m}) \right\} + \{T(\partial p/\partial T)_{sat}\, (dV_m(l)/dT)\} \qquad (11)$$

Thus, reliable liquid-density values are also required to determine $C_{sat,m}$.

Table 11 lists the experimental two-phase heat capacities $C^{II}_{x,m}$ for benzothiazole and benzoxazole obtained for three cell fillings for each compound. Heat capacities were determined at 20-K intervals with a heating rate of $0.083\ K \cdot s^{-1}$ and a 120-s equilibration period between heats. Sample decomposition precluded heat-capacity measurements above 600 K for benzothiazole and 665 K for benzoxazole.

For other compounds studied recently at NIPER, e.g., dibenzothiophene[50] and 2-aminobiphenyl,[51] a single continuous heat at a rate of $0.333\ K\ s^{-1}$ was used, sample decomposition was greatly reduced, and the abrupt decrease in heat capacity associated with the conversion from two phases to one phase was observed. For dibenzothiophene and 2-aminobiphenyl, temperatures at which conversion to the single phase occurred were measured in this way for six cell fillings, and critical temperatures and densities were derived graphically. For benzothiazole, decomposition began far below the estimated T_c, and this method was not applicable. For benzoxazole, decomposition started within 30 K of the estimated T_c, and it was seldom possible to observe evidence for the two-phase to one-phase conversion, even when rapid heating rates were used. For two cell fillings only, near the critical-density estimate

(described earlier), it was possible to observe the sudden decrease in observed heat capacity associated with conversion to a single phase superimposed on the effects of sample decomposition. The conversion temperature for both fillings was 695 K, which was assumed to be the critical temperature. The uncertainty in this value is difficult to assess, but is estimated to be 5 K.

The critical pressure for benzoxazole was not measured directly, but was estimated by a simultaneous non-linear least-squares fit of the vapor pressures listed in table 4 and the $C^{II}_{x,m}$ values given in table 11. $C_{sat,m}$ values were derived from results of the fit and equation (**11**). Experimental $C^{II}_{x,m}$ were converted to $C^{II}_{v,m}$ values by means of equation (**9**) for the cell expansion and the vapor-pressure fit described below for $(\partial p/\partial T)_{sat}$. The relevant equation is:

$$C^{II}_{v,m} = C^{II}_{x,m} - T/n \{(\partial V_x/\partial T)_x (\partial p/\partial T)_{sat}\}. \qquad (12)$$

The values of $C^{II}_{v,m}$ were used to derive functions for $(\partial^2 p/\partial T^2)_{sat}$ and $(\partial^2 \mu/\partial T^2)_{sat}$. The Cox equation[38] was used to represent the vapor pressures in the form:

$$\ln(p/p_c) = (1 - 1/T_r) \exp (A + BT_r + CT_r^2), \qquad (13)$$

with $T_r = T/T_c$, where T_c and p_c are the critical temperature and critical pressure. The critical pressure was included as a variable in the non-linear least-squares analysis. The functional form chosen for variation of the second derivative of the chemical potential with temperature was:

$$(\partial^2 \mu/\partial T^2)_{sat} = \sum_{i=0}^{n} b_i (1 - T/T_c)^i. \qquad (14)$$

{For compounds where sufficient information was available to evaluate reliably $(\partial^2 \mu/\partial T^2)_{sat}$ (e.g., benzene[52]), four terms (i.e, expansion to n=3) were required to represent the function. Thus, four terms were used in this research.} In these fits the sum of the weighted squares in the following function was minimized:

$$\Delta = C^{II}_{v,m}/R - \{V_m(l)T/nR\}(\partial^2 p/\partial T^2)_{sat} + (T/R)(\partial^2 \mu/\partial T^2)_{sat}. \qquad (15)$$

For the vapor-pressure fits, the functional forms of the weighting factors used have been reported.[30] Within the heat-capacity results, the weighting factors were proportional to the square of the mass of sample used in the measurements. Table 12 lists the coefficients determined in the non-linear least-squares fit. A weighting factor

of 20 was used to increase the relative weights of the vapor-pressure measurements in the fit. The weighting factor reflects the higher precision of the vapor-pressure values relative to the experimental heat capacities.

Values of $C_{sat,m}$ for benzothiazole were determined with equation (**11**). Values of $(\partial p/\partial T)_{sat}$ were calculated with the Cox parameters listed in table 5, and values of $(dV_m(l)/dT)$ were derived with equation (**7**). Values of the term involving $C^{II}_{V,m}$ were determined with equation (**12**). The calculations were for temperatures sufficiently removed from T_c to allow use of estimated critical parameters without detriment to the accuracy of the derived C_{sat} values. Values of $C_{sat,m}$ and $C^{II}_{V,m}(\rho=\rho_{sat})$ for benzoxazole and benzothiazole are listed in table 13.

THERMODYNAMIC PROPERTIES IN THE CONDENSED STATE

Entropies and enthalpies under vapor saturation pressure relative to that of the crystals at $T\rightarrow 0$ for the solid and liquid phases of benzothiazole and benzoxazole are listed in table 10. The tabulated values were derived by integration of the smoothed heat capacities corrected for pre-melting, together with the entropies and enthalpies of transition and fusion. The heat capacities were smoothed with cubic-spline functions by least-squares fits to six points at a time and by requiring continuity in value, slope, and curvature at the junction of successive cubic functions. Due to limitations in the spline-function procedure, some acceptable values from tables 9 and 13 were not included in the fit, while in other regions graphical values were introduced to ensure that the second derivative of the heat capacity with respect to temperature was a smooth function of temperature. Pre-melting corrections were made by means of standard methods[47] for solid-insoluble impurities and the mole-fraction impurities values shown in table 1.

THERMODYNAMIC PROPERTIES IN THE IDEAL-GAS STATE

Enthalpies and entropies at selected temperatures for the ideal gas for benzothiazole and benzoxazole were calculated using values in tables 6 and 10 and are listed in columns 2 and 4 of table 14. Entropies and enthalpies of compression to 101.325 kPa were calculated based on the virial equation truncated after the third virial coefficient,

$$pV_m = RT + Bp + Cp^2 \ . \qquad (16)$$

Formulations used to calculate the entropy and enthalpy of compression are:[53]

$$\Delta S_{comp,m} = R\ \ln(p) + (dB/dT)p + (dC/dT)p^2 \ , \qquad (17)$$

$$\Delta H_{comp,m} = \{B - T(dB/dT)\}p + \{C - T(dC/dT)\}(p^2/2). \quad (18)$$

Equations (17) and (18) are derived from equations (16.21) and (16.27), respectively, of reference 53. Temperature derivatives were estimated by numerical differentiation of virial coefficients estimated by the methods of Pitzer and Curl[44] and Orbey and Vera.[45]

The first term in equation (17) is the entropy of compression, if the gas were ideal. The uncertainty in this term is not significant. The sum of the second and third terms of equation (17) is the "gas-imperfection correction" to the entropy of compression. Equation (18) gives the "gas-imperfection correction" to the enthalpy of compression directly, as the enthalpy of compression for an ideal-gas is zero. The gas-imperfection corrections are listed in columns 3 and 5, and are included in columns 2 and 4 of table 14. Uncertainties in these values are difficult to assess because temperature derivatives of estimated values are involved. An uncertainty of 10 per cent of the calculated correction was assumed.

The derived ideal-gas enthalpies and entropies were combined with the condensed-phase enthalpies of formation given in table 3 to calculate the enthalpies, entropies, and Gibbs energies of formation listed in columns 6, 7, and 8, respectively, of table 14. Enthalpies and entropies for $N_2(g)$, $S_2(g)$, and equilibrium hydrogen were derived from from JANAF tables.[54] Values for graphite were determined with the polynomial[55] used to calculate the values from 298.15 K to 6000 K listed in the JANAF tables. All uncertainties in table 14 represent one standard deviation and do not include uncertainties in the properties of the elements. Uncertainties in the properties of the elements were not included because they cancel in calculations of chemical equilibria. Their inclusion would lead to overestimation of the error limits in such calculations.

CALCULATION OF SUBLIMATION PRESSURES

The "third-law" method was employed to calculate sublimation pressures for benzoxazole from 280 K to T_{tp}. The "third-law" values were calculated from the tabulated thermodynamic functions of the ideal gas (table 14) and the crystalline solid (table 10). The method applied here was the same as that used previously for biphenyl.[49] The sublimation vapor pressures were represented by the equation:

$$\ln(p/p_o) = 31.13 - 7490(T/K)^{-1} - 1.276\times10^5(T/K)^{-2}, \quad (19)$$

in the temperature region 280 K to 302.5 K with p_o = 1 Pa.

4. DISCUSSION

BENZOXAZOLE SUBLIMATION PRESSURES

Vapor pressures for both the supercooled liquid and the cr(I) phase for benzoxazole were obtained as part of the inclined-piston vapor-pressure measurements. The measured values are reported in table 4 and marked by footnotes. (The supercooled-liquid values were included in the fitting procedure to obtain the Cox-equation parameters listed in table 5.)

Table 15 lists the measured sublimation pressures, vapor pressures calculated with the Cox equation parameters listed in table 5, and sublimation pressures calculated by means of the "third law" method (equation **19**). The difference between the measured and calculated sublimation pressures (column 5 of table 15) is nearly constant at 1 Pa. This difference, though small, is a significant percentage of the pressure at the lowest temperature of the measurements and is five times the assigned uncertainty of 0.2 Pa. The deviation probably arises from incomplete outgassing of the system during the inclined-piston measurements. This illustrates the difficulty in making low-pressure measurements in a static system, even when special outgassing techniques are used. At the triple point (302.505 K), both equation (**19**) and the Cox-equation parameters listed in table 5 give a vapor pressure of 144.9 Pa for benzoxazole.

COMPARISON OF RESULTS WITH LITERATURE

Vapor pressures of benzothiazole were measured at three temperatures (433.4 K, 453.5 K, and 473.5 K) by Krevor et al.[56] as part of a (vapor+liquid) equilibrium (VLE) study. Their values relative to those of this research are approximately 1.5 per cent high, which is in accord with the expected accuracy of their measurements.

In this paper the events in the heat-capacity curves near 246 K are termed "phase transitions." The nature of the structural changes associated with these events is unknown. Crystal structures determined by x-ray crystallography above and below T_{trs} may or may not show a clear difference. The structural change may be associated with a subtle event, such as the freeing of a molecular vibration, which is restricted in the low-temperature form.

Heat capacities and enthalpies of benzothiazole were measured previously from 5 K to 320 K by Goursot and Westrum.[57] The purity of their sample (0.9990), as determined by fractional melting, was slightly lower than that of the sample used in this research (0.9999). Figure 5 is a deviation plot for the heat capacities determined by Goursot and Westrum from those of this research for the liquid phase and for phase

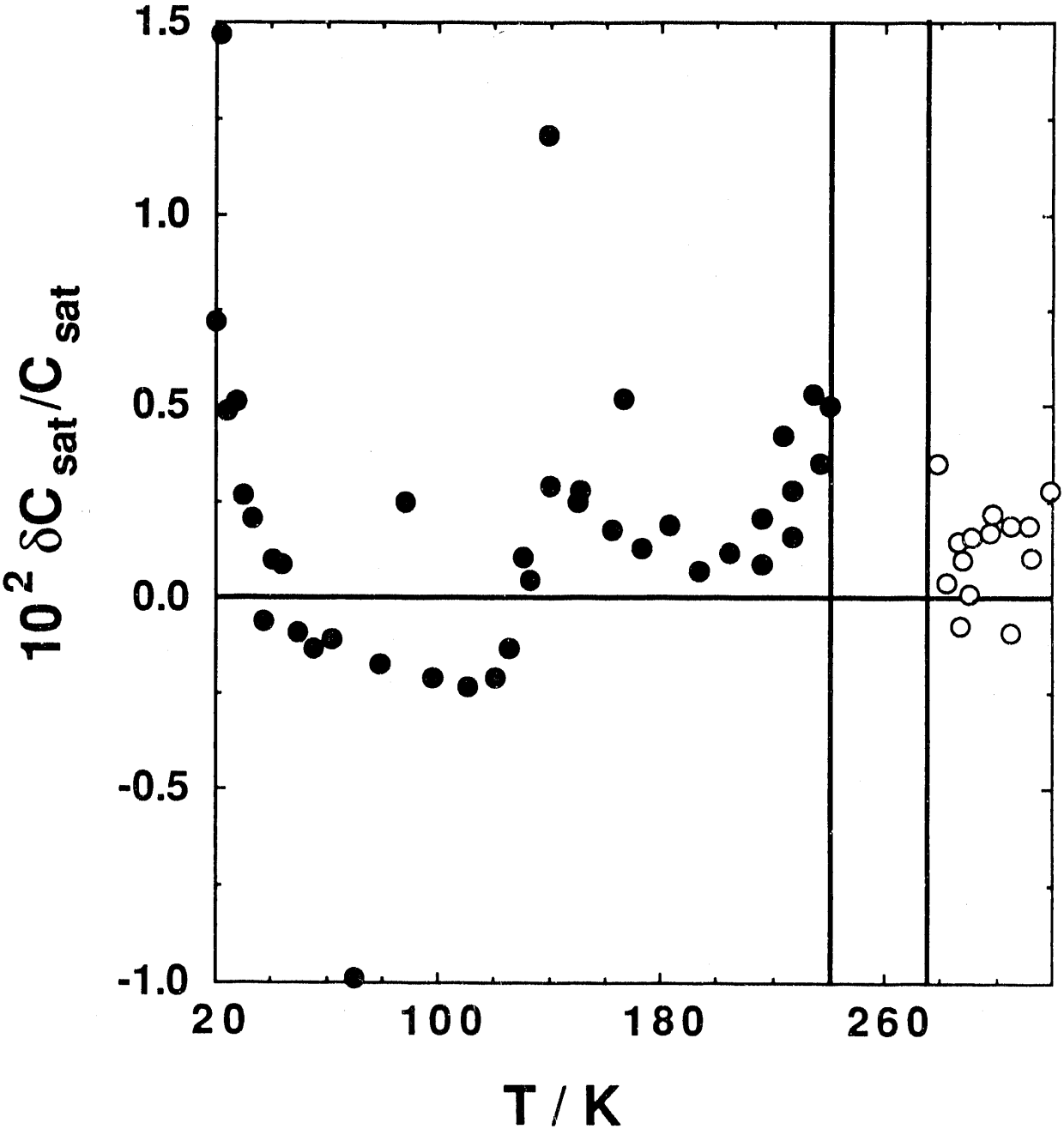

FIGURE 5. Percentage deviations $10^2\delta C_{sat}/C_{sat}$ of the heat capacities of benzothiazole measured by Goursot and Westrum[57] for the crystalline phase between 20 K and 240 K and the liquid phase above 275 K. The vertical lines indicate phase-transition temperatures of this research.

cr(II) between 20 K and 240 K. Comparison with their results for phase cr(I) is not made because their results in this temperature region are complicated by the presence of significant premelting, as seen in figure 3. Goursot and Westrum do not report the temperature increments associated with their average heat-capacity measurements. Consequently, the premelting correction cannot be calculated.

Goursot and Westrum did not observe the conversion from cr(II) to cr(I) in the heat-capacity curve near 245 K. Their results near 245 K are represented in figure 3 by the unfilled triangles. It is seen in the figure that the series 14 result of our research, which was obtained after a relatively short annealing time near 240 K, is in good accord with the results of Goursot and Westrum. It seems probable that they failed to observe the cr(II) to cr(I) change in the heat-capacity curve because their sample was insufficiently annealed. Goursot and Westrum do not mention equilibration times, so no comparison can be made in this area.

Goursot and Westrum measured the enthalpy of fusion ten times and reported an average enthalpy increment from 240 K to 280 K, $\{H^{l}_{m}(280\ K) - H^{s}_{m}(240\ K)\}/RK = (2177.4)$. The corresponding value from the results of the present research is $\{H^{l}_{m}(280\ K) - H^{s}_{m}(240\ K)\}/RK = (2182.8)$. This difference is consistent with Goursot and Westrum having failed to convert their sample from cr(I) to cr(II). The difference in $\Delta_{trs}H_m/RK$ for series 13 (annealed 11 d) and series 14 (annealed 0.8 d) of this research (5.7) is in good accord with the difference between the 240 K-to-280 K enthalpy increments (5.4).

The crystal-phase enthalpy increment between 240 K and T_{tp} reported by Goursot and Westrum is inexplicably low. Hence, their calculated enthalpy of fusion is anomalously high. The value for T_{tp} (275.65 K) reported by Goursot and Westrum agrees with that reported here.

Kambe and Yokota[58] reported values for the enthalpy of fusion determined by d.s.c. for benzothiazole and benzoxazole, which are 8 per cent and 20 per cent low, respectively, relative to the values obtained in this research. Meyer and Metzger[59] reported a value determined by cooling-curve analysis for the enthalpy of fusion of benzothiazole, which is 6 per cent higher than the present result.

Goursot and Westrum,[57] Meyer and Metzger,[59] and Witschonke[60] have reported the existence of a lower-melting metastable phase for benzothiazole. This phase was not detected in our research.

A complete spectral assignment was published by Mille et al.[61] for benzoxazole and by Panizzi et al.[62] for benzothiazole. These publications are from the same research group. The rigid-rotor and harmonic-oscillator approximations were used to

calculate the ideal-gas entropies for the temperature ranges studied calorimetrically in this research. The moment of inertia products for benzothiazole (1.3021×10^{-133} $kg^3 \cdot m^6$) and benzoxazole (6.3575×10^{-134} $kg^3 \cdot m^6$) were calculated with structures determined with the molecular mechanics program MMP2.[63]

Differences between the spectroscopic and calorimetrically-derived ideal-gas entropies are shown in figure 6. Values based on the spectral assignments for both compounds are low by 0.6R to 1.0R relative to the calorimetric values. This is nearly identical to the results obtained previously for benzo[b]furan and benzothiophene.[64,65] (Mille et al.[66] also published complete assignments for benzo[b]furan and benzo[b]thiophene.) For benzo[b]furan, it was shown by Collier[67] and Smithson et al.[68] that two fundamental vibrations were present below 400 cm^{-1} (at 211 cm^{-1} and 246 cm^{-1}), while Mille et al.[66] assigned one to a fundamental and the second to a difference band. Furthermore, Collier concluded that the band at 583 cm^{-1}, assigned as a fundamental by Mille et al.,[66] was a combination band. Ideal-gas entropies based on the results of Collier[67] were in excellent accord with the calorimetric results for benzo[b]furan.

For benzothiazole, Panizzi et al.[62] observed two bands in their liquid-phase vibrational spectra (near 202 cm^{-1} and 220 cm^{-1}) and assigned one (at 202 cm^{-1}) to a fundamental and the second to a difference band. Analogously for benzoxazole, Mille et al.[61] observed two bands in their liquid-phase vibrational spectra (near 226 cm^{-1} and 259 cm^{-1}) and assigned only one (at 226 cm^{-1}) to a fundamental. Because of wavenumber shifts caused by intermolecular interactions, wavenumber values from vapor-phase spectra are preferred for the vibrational assignments. (For example, Collier[67] found significant liquid-to-vapor shifts in the two lowest nonplanar modes for benzo[b]furan. The observed frequencies in the liquid phase were 225 cm^{-1} and 257 cm^{-1} which shifted to 211 cm^{-1} and 246 cm^{-1} in the gas phase.) The vapor-phase spectra published by Panizzi et al.,[62] are insufficiently resolved to accurately assign the lowest-wavenumber fundamentals. Reassignments of the benzothiazole and benzoxazole spectra are being completed at NIPER.

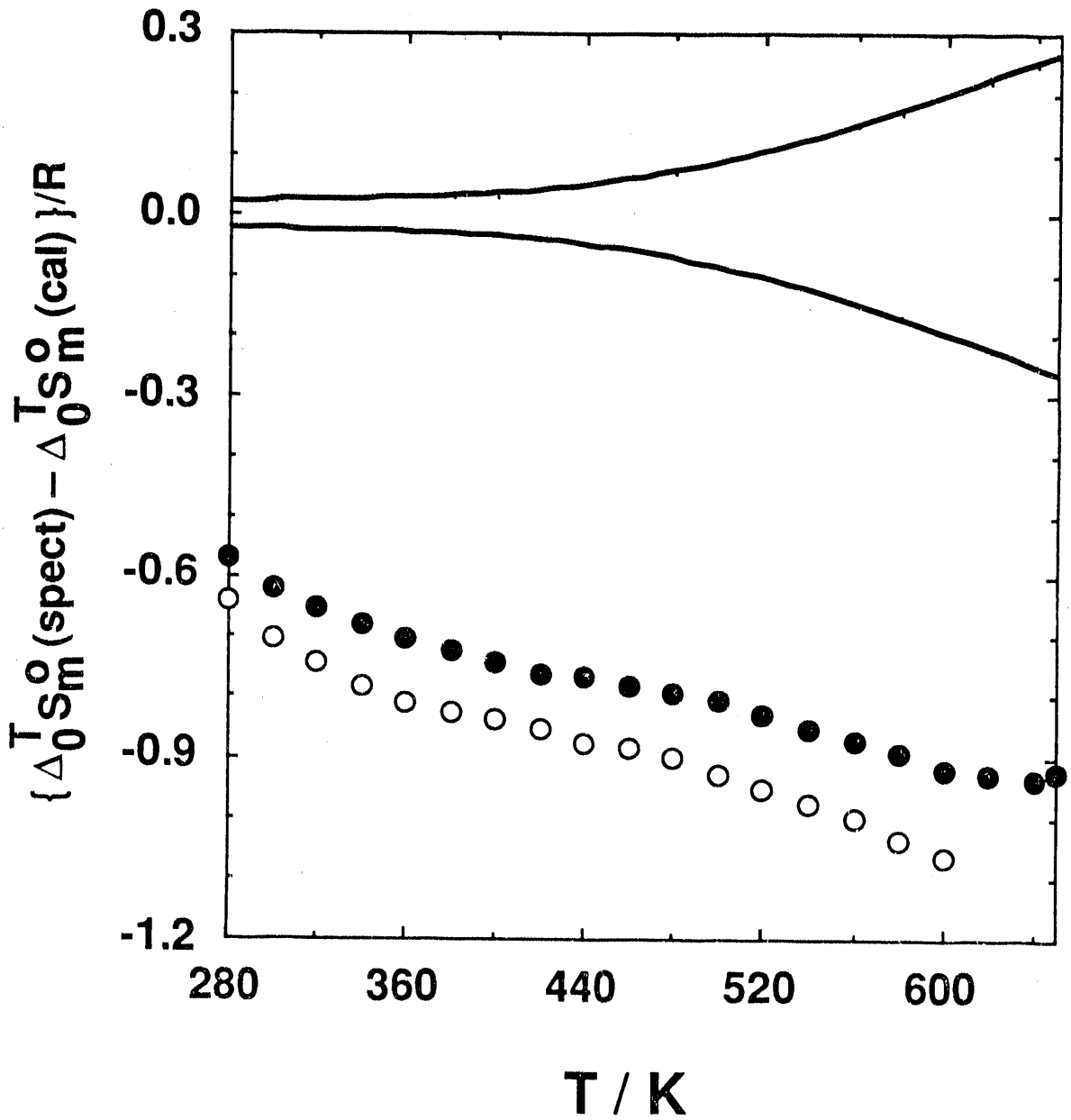

FIGURE 6. Deviation of ideal-gas entropy values calculated from spectroscopically determined vibrational frequencies and statistical mechanics (spect) from the calorimetrically (cal) derived values of this research. The curved lines represent the uncertainty limits of the calorimetric results (one standard deviation). The curve defined by ● is based on the spectroscopic results of Mille et al.[61] for benzoxazole. The curve defined by ○ is based on the spectroscopic results of Panizzi et al.[62] for benzothiazole.

5. SUMMARY and HIGHLIGHTS

- Thermochemical and thermophysical properties for diheteroatom compounds benzothiazole and benzoxazole are reported. Properties measured included vapor pressures and heat capacities over a range of temperatures, and the energy of combustion.

- Gibbs energies of formation for benzothiazole and benzoxazole for equilibria calculations were derived. The determination of these is an essential precursor to a thermodynamic analysis of the initial steps of the hydrogenolysis of these materials, which will be presented in a subsequent topical report.

- Ideal-gas thermodynamic properties for benzothiazole and benzoxazole were determined based on the accurate calorimetric measurements. These are the first for diheteroatom-containing compounds, and will provide the basis for group-contribution parameters for previously undefined groups.

- Published vibrational assignments for benzothiazole and benzoxazole appear to be in error with regard to assignment of the lowest-wavenumber modes. A new assignment is being developed at NIPER.

6. REFERENCES

1. Odebunmi, E. O.; Ollis, D. F. *J. Catalysis* **1983**, 80, 65.
2. Nagai, M.; Kabe, T. *J. Catalysis* **1983**, 81, 440.
3. Nagi, M.; Sato, T.; Aiba, A. *J. Catalysis* **1986**, 97, 52.
4. Girgis, M. J. *Reaction Networks, Kinetics, and Inhibition in the Hydroprocessing of Simulated Heavy Coal Liquids* PhD Thesis University of Delaware, **1988**.
5. Steele, W. V.; Chirico, R. D.. *Thermodynamics and the Hydrodenitrogenation of Indole. In three parts: Part I. Thermodynamic Properties of Indoline and 2-Methylindole, Part II. Gibbs Energies of Reaction in the Hydrodenitrogenation of Indole, Part III. Thermodynamic Equilibria and Comparison with Literature Kinetic Studies.* NIPER-415. Published by DOE Fossil Energy, Bartlesville Project Office. Available from NTIS, Report No. DE-89000751, June **1989**.
6. Geneste, P.; Amblard, P.; Bonnet, M.; Graffin, P. *J. Catalysis* **1980**, 61, 115.
7. Konuma, K.; Hasegawa, H.; Itabashi, K. *Nippon Kagaku Kaishi* **1984**, 592.
8. Konuma, K.; Hasegawa, H.; Itabashi, K. *Applied Catalysis* **1988**, 38, 109.
9. Konuma, K.; Hasegawa, H.; Itabashi, K. *Nippon Kagaku Kaishi* **1986**, 1771.
10. Fan, W.; Yang, Q. *Ranliao Huaxue Xuebao* **1988**, 16, 237.
11. Commission on Atomic Weights and Isotopic Abundances. *Pure Appl. Chem.* **1983**, 55, 1101.
12. Cohen, E. R.; Taylor, B. N. *J. Phys. Chem. Ref. Data* **1988**, 17, 1795.
13. *Metrologia* **1969**, 5, 35.
14. McCrackin, F. L.; Chang, S. S. *Rev. Sci. Instrum.* **1975**, 46, 550.
15. Good, W. D.; Moore, R. T. *J. Chem. Eng. Data* **1970**, 15, 150.
16. Good, W. D.; Smith, N. K. *J. Chem. Eng. Data* **1969**, 14, 102.
17. Good, W. D. *J. Chem. Eng. Data* **1969**, 14, 231.
18. Good, W. D. *J. Chem. Eng. Data* **1972**, 17, 158.
19. Good, W. D.; Scott, D. W.; Waddington, G. *J. Phys. Chem.* **1956**, 60, 1080.
20. Good, W. D.; Douslin, D. R.; Scott, D. W.; George, A.; Lacina, J. L.; McCullough, J. P.; Waddington, G. *J. Phys. Chem.* **1959**, 63, 1133.
21. Smith, N. K.; Stewart, R. C., Jr.; Osborn, A. G.; Scott, D. W. *J. Chem. Thermodynamics* **1980**, 12, 919.
22. Chirico, R. D.; Hossenlopp, I. A.; Nguyen, A.; Strube, M. M.; Steele, W. V. *Thermodynamic Studies Related to the Hydrogenation of Phenanthrene.* NIPER-247. Published by DOE Fossil Energy, Bartlesville Project Office. Available from NTIS Report No. DE-87001252, April **1987**.
23. Goldberg, R. N.; Nuttall, R. N.; Prosen, E. J.; Brunetti, A. P. *NBS Report 10437,* U. S. Department of Commerce, National Bureau of Standards, June **1971**.
24. Swietoslawski, W. *Ebulliometric Measurements.* Reinhold: New York, **1945**.
25. Osborn A. G.; Douslin, D. R. *J. Chem. Eng. Data* **1966**, 11, 502.

26. Chirico, R. D.; Nguyen, A.; Steele, W. V.; Strube, M. M.; Tsonopoulos, C. *J. Chem. Eng. Data* **1989**, 34, 149.
27. Antoine, C. *C. R. Acad. Sci.* **1888**, 107, 681.
28. Douslin, D. R.; McCullough, J. P. *U. S. Bureau of Mines. Report of Investigation 6149*, **1963**, pp. 11.
29. Douslin, D. R.; Osborn A. G. *J. Sci. Instrum.* **1965**, 42, 369.
30. Steele, W. V.; Archer, D. G.; Chirico, R. D.; Collier, W. B.; Hossenlopp, I. A.; Nguyen, A.; Smith, N. K.; Gammon, B. E. *J. Chem. Thermodynamics* **1988**, 20, 1233.
31. Steele, W. V.; Chirico, R. D.; Knipmeyer, S. E.; Smith, N. K. *High-Temperature Heat-Capacity Measurements and Critical Property Determinations using a Differential Scanning Calorimeter. (Development of Methodology and Application to Pure Organic Compounds)* NIPER-360. Published by DOE Fossil Energy, Bartlesville Project Office. Available from NTIS, Report No. DE89000709, December **1988**.
32. Knipmeyer, S. E.; Archer, D. G.; Chirico, R. D.; Gammon, B. E.; Hossenlopp, I. A.; Nguyen, A.; Smith, N. K.; Steele, W. V.; Strube, M. M. *Fluid Phase Equilibria* **1989**, 52, 185.
33. Mraw, S. C.; Naas, D. F. *J. Chem. Thermodynamics* **1979**, 11, 567.
34. Hubbard, W. N.; Scott, D. W.; Waddington, G. *Experimental Thermochemistry*. Rossini, F. D.: editor. Interscience: New York, **1956**, Chapt. 5, pp. 75-128.
35. Hubbard, W. N.; Katz, C.; Waddington, G. *J. Phys. Chem.* **1954**, 58, 142.
36. Rossini, F. D. *Experimental Thermochemistry*. Rossini, F. D.: editor. Interscience: New York. **1956**, Chapt. 14, pp. 297-320.
37. Cox, J. D.; Wagman, D. D.; Medvedev, V. A.: editors. *CODATA Key Values for Thermodynamics*. Hemisphere: New York. **1989**.
38. Cox, E. R. *Ind. Eng. Chem.* **1936**, 28, 613.
39. Joback, K. G. *S. M. Thesis*. Massachusetts Institute of Technology:Cambridge, MA. **1984**. The equations and parameters are listed in reference 40.
40. Reid, R. C.; Prausnitz, J. M.; Poling, B. E. *The Properties of Liquids and Gases*. 4th edition. McGraw-Hill: New York. **1987**.
41. Somayajulu, G. R. *J. Chem. Eng. Data* **1989**, 34, 106.
42. Riedel, L. *Chem.-Ing.-Tech* **1954**, 26, 259.
43. Hales, J. L.; Townsend, R. *J. Chem. Thermodynamics* **1972**, 4, 763.
44. Pitzer, K. S.; Curl, R. F. Jr. *J. Am. Chem. Soc.* **1957**, 79, 2369.
45. Orbey, H.; Vera, J. H. *AIChE Journal*, **1983**, 29, 107.
46. Steele, W. V.; Chirico, R. D. To be published.
47. Westrum, E. F., Jr.; Furukawa, G. T.; McCullough, J. P. *Experimental Thermodynamics*. Vol. 1. McCullough, J. P.; Scott, D. W.: editors. Butterworths: London. **1968**, Chapt 5.

48. Mastrangelo, S. V. R.; Dornte, R. W. *J. Am. Chem. Soc.* **1955**, 77, 6200.
49. Chirico, R. D.; Knipmeyer, S. E.; Nguyen, A.; Steele, W. V. *J. Chem. Thermodynamics* **1989**, 21, 1307.
50. Chirico, R. D.; Knipmeyer, S. E.; Nguyen, A.; Steele, W. V. *J. Chem. Thermodynamics* **1991**, 23, 431.
51. Steele, W. V.; Chirico, R. D.; Knipmeyer, S. E.; Nguyen, A. *The Thermodynamic Properties of 2-Aminobiphenyl. (An Intermediate in the Carbazole/Hydrogen Reaction Network).* NIPER-482. Published by DOE Fossil Energy, Bartlesville Project Office. Available from NTIS, Report No. DE-91002209, December **1990**.
52. Goodwin, R. D. *J. Phys. Chem. Ref. Data* **1988**, 17, 1541.
53. Lewis, G. N.; Randall, M. *Thermodynamics.* Revised by Pitzer, K. S.; Brewer, L. 2nd edition. McGraw-Hill: New York. **1961**.
54. Chase, M. W., Jr.; Davies, C. A.; Downey, J. R.; Frurip, D. J.; McDonald, R. A.; Syverud, A. N. *JANAF Thermochemical Tables* Third edition. Supplement to *J. Phys. Chem. Ref. Data* **1985**, 14.
55. Chirico, R. D.; Archer, D. G.; Hossenlopp, I. A.; Nguyen, A.; Steele, W. V.; Gammon, B. E. *J. Chem. Thermodynamics* **1990**, 22, 665.
56. Krevor, D. H.; Lam, F. W.; Prausnitz, J. M. *J. Chem. Eng. Data* **1986**, 31, 353.
57. Goursot, P.; Westrum, E. F., Jr. *J. Chem. Eng. Data* **1969**, 14, 1.
58. Kambe,H.; Yokota, R. *Anal. Calorimetry* **1974**, 3, 621.
59. Meyer, R.; Metzger, J. *Ann. Fac. Sci. Marseille* **1964**, 35, 33.
60. Witschonke, C. R. *Anal. Chem.* **1954**, 26, 562.
61. Mille, G.; Davidovics, G.; Chouteau, J. *C. R. Acad. Sci.* **1972**, 274, 532.
62. Panizzi, J-C.; Davidovics, G.; Guglielmetti, R.; Mille, G.; Metzger, J.; Chouteau, J. *Can. J. Chem.* **1971**, 49, 956.
63. Burkert, U.; Allinger N. L. *Molecular Mechanics* Amer. Chem. Soc.: Washington D.C. **1982**.
64. Steele, W. V.; Chirico, R. D. *Thermodynamics and the Hydrodeoxygenation of 2,3-Benzofuran* NIPER-457. Published by DOE Fossil Energy, Bartlesville Project Office. Available from NTIS, Report No. DE-90000218, February **1990**.
65. Chirico, R. D.; Knipmeyer, S. E.; Nguyen, A.; Steele, W. V. *The Thermodynamic Properties of Benzothiophene* NIPER-509. Published by DOE Fossil Energy, Bartlesville Project Office. Available from NTIS, Report No. DE-91002218, January **1991**.
66. Mille, G.; Davidovics, G.; Chouteau, J. *J. Chim. Phys. Physicochim. Biol.* **1972**, 69, 1662.
67. Collier, W. B. *J. Chem. Phys.* **1988**, 88, 7295.
68. Smithson, T. L.; Shaw, R. A.; Wieser, H. *J. Chem. Phys.* **1984**, 81, 4281.

TABLE 1. Calorimeter and sample characteristics for adiabatic heat-capacity calorimetry studies: m is the sample mass; V_i is the internal volume of the calorimeter; T_{cal} is the temperature of the calorimeter when sealed; p_{cal} is the pressure of the helium and sample when sealed; r is the ratio of the heat capacity of the full calorimeter to that of the empty; T_{max} is the highest temperature of the measurements; and $\delta C/C$ is the vaporization correction; x_{pre} is the mole-fraction impurity used for pre-melting corrections.

	Benzothiazole	**Benzoxazole**
	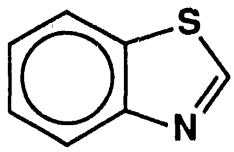	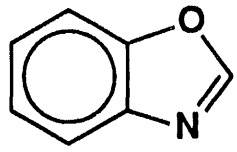
m/g	57.847	54.185
V_i(298.15 K)/cm^3	59.06	59.06
T_{cal}/K	299.2	301.7
p_{cal}/kPa	4.48	4.40
r(T_{max})	3.3	3.4
r_{min}	1.9	1.9
$10^2 \cdot (\delta C/C)_{max}$	0.028	0.061
x_{pre}	0.0	0.00031

TABLE 2. Typical combustion experiment at 298.15 K for benzothiazole and benzoxazole. (p° = 101.325 kPa) [a]

	Benzothiazole	Benzoxazole
m'(compound)/g	1.215220	1.038341
m''(fuse)/g	0.001143	0.001074
m'''(oil)/g	0.027793	0.075611
$n_i(H_2O)$/mol	0.5535	0.05535
m(Pt)/g	20.809	20.203
$\Delta T=(t_i - t_f + \Delta t_{corr})$/K	2.33154	2.00488
ε(calor)(ΔT)/J	−39104.6	−33627.9
ε(cont)(ΔT)/J [b]	−131.8	−38.3
ΔU_{ign}/J	0.8	0.8
$\Delta U_{dec}(HNO_3)$/J	74.0	116.3
$\Delta U_{dil}(H_2SO_4)$/J [c]	−6.4	0.0
ΔU(corr. to std. states)/J [d]	30.5	23.2
$-m''(\Delta_c U^\circ_m/M)$(fuse)/J	19.4	18.2
$m'''(\Delta_c U^\circ_m/M)$(oil)/J	−1279.7	−3481.3
$m'(\Delta_c U^\circ_m/M)$(compound)/J	−37838.4	−30026.4
$(\Delta_c U^\circ_m/M)$(compound)/J·g^{-1}	−31137.1	−28917.7

a The symbols and abbreviations of this table are those of reference 34 except as noted.

b ε_i(cont)(t_i − 298.15 K) + ε_f(cont)(298.15 K − t_f + Δt_{corr}).

c Dilution of sulfuric acid formed to the standard state $H_2SO_4 \cdot 115H_2O$.

d Items 81 to 85, 87 to 90, 93, and 94 of the computational form of reference 34.

TABLE 3. Summary of energies of combustion and molar thermochemical functions for benzothiazole and benzoxazole. (T = 298.15 K and p° =101.325 kPa)

$\{(\Delta_c U^\circ_m/M)(\mathbf{Benzothiazole})\}/(J\cdot g^{-1})$	
−31137.1 −31138.2 −31136.2 −31139.8 −31135.5	
$\langle\{(\Delta_c U^\circ_m/M)(\mathbf{Benzothiazole})\}/(J\cdot g^{-1})\rangle$	−31137.4±0.8
$(\Delta_c U^\circ_m)(\mathbf{Benzothiazole})/(kJ\cdot mol^{-1})$	−4209.57±0.56
$(\Delta_c H^\circ_m/M)(\mathbf{Benzothiazole})/(kJ\cdot mol^{-1})$	−4215.15±0.56
$(\Delta_f H^\circ_m/M)(\mathbf{Benzothiazole})/(kJ\cdot mol^{-1})$	144.03±0.70 [a]
$(\Delta_f H^\circ_m/M)(\mathbf{Benzothiazole})/(kJ\cdot mol^{-1})$	75.79±0.76 [b]
$\{(\Delta_c U^\circ_m/M)(\mathbf{Benzoxazole})\}/(J\cdot g^{-1})$	
−28917.7 −28921.8 −28903.5 −28917.1	
−28911.4 −28928.1 −28914.2 −28899.6	
$\langle\{(\Delta_c U^\circ_m/M)(\mathbf{Benzoxazole})\}/(J\cdot g^{-1})\rangle$	−28914.2±3.8
$(\Delta_c U^\circ_m)(\mathbf{Benzoxazole})/(kJ\cdot mol^{-1})$	−3444.34±1.00
$(\Delta_c H^\circ_m/M)(\mathbf{Benzoxazole})/(kJ\cdot mol^{-1})$	−3444.96±1.00
$(\Delta_f H^\circ_m/M)(\mathbf{Benzoxazole})/(kJ\cdot mol^{-1})$	−24.19±1.05 [c]

a For the reaction 7 C (cr, graphite) + 2.5 H_2 (g) + 0.5 N_2 (g) + S (cr, rhombic) = C_7H_5NS (l)

b For the reaction 7 C (cr, graphite) + 2.5 H_2 (g) + 0.5 N_2 (g) + 0.5 S_2 (g) = C_7H_5NS (l)

c For the reaction 7 C (cr, graphite) + 2.5 H_2 (g) + 0.5 N_2 (g)+ 0.5 O_2 (g) = C_7H_5NO (cr).

TABLE 4. Vapor-pressure results: IP refers to measurements performed with the inclined-piston gauge; water or decane refers to which material was used as the standard in the reference ebulliometer; T is the temperature of the experimental inclined-piston pressure gauge measurements or, for ebulliometric measurements, of the condensation temperature of the sample; the pressure p for ebulliometric measurements was calculated from the condensation temperature of the reference substance; Δp is the difference of the calculated value of pressure from the observed value of pressure; σ_i is the propagated error calculated from equations (1) and (2); ΔT is the difference between the boiling and condensation temperatures ($T_{boil} - T_{cond}$) for the sample in the ebulliometer

Method	T / K	p / kPa	Δp / kPa	$\sigma(p)$ / kPa	ΔT / K
		Benzothiazole			
IP	305.005	0.0191	0.0001	0.0002	
IP	315.005	0.0400	0.0002	0.0002	
IP	325.001	0.0792	0.0000	0.0002	
IP	335.002	0.1507	0.0004	0.0002	
IP	345.005	0.2736	0.0005	0.0002	
IP	355.001 [a]	0.4770	0.0004	0.0003	
IP	355.000	0.4769	0.0004	0.0003	
IP	365.003	0.8027	0.0007	0.0003	
IP	375.002	1.3062	0.0009	0.0004	
decane	384.325	2.0000	−0.0003	0.0001	0.086
IP	385.004	2.0628	0.0013	0.0005	
decane	390.927	2.6660	−0.0002	0.0002	0.067
decane	408.048	5.3330	0.0002	0.0003	0.043
decane	418.940	7.9989	0.0001	0.0004	0.036
decane	427.113	10.6661	−0.0002	0.0006	0.041
decane	433.721	13.332	0.000	0.001	0.039
decane	440.585	16.665	0.001	0.001	0.039
decane	446.292	19.933	−0.001	0.001	0.037
decane	453.798	25.023	0.001	0.001	0.036
water	453.785 [a]	25.023	0.010	0.001	0.042
water	461.356	31.177	0.001	0.002	0.040
water	468.962	38.565	0.004	0.002	0.037

TABLE 4. Continued

Method	T / K	p / kPa	Δp / kPa	σ(p) / kPa	ΔT / K
water	476.624	47.375	−0.002	0.002	0.034
water	484.331	57.817	−0.002	0.003	0.037
water	492.087	70.120	0.000	0.003	0.038
water	499.898	84.533	−0.005	0.004	0.034
water	507.756	101.325	−0.004	0.004	0.035
water	515.662	120.790	0.002	0.005	0.037
water	523.622	143.250	0.008	0.006	0.040
water	531.629	169.02	0.01	0.01	0.045
water	539.689	198.49	0.01	0.01	0.050
water	547.797	232.02	0.00	0.01	0.059
water	555.953	270.02	−0.02	0.01	0.073
		Benzoxazole			
IP	280.003 [b]	0.0165		0.0002	
IP	284.999 [b]	0.0275		0.0002	
IP	290.001 [b]	0.0450		0.0002	
IP	295.001 [b]	0.0728		0.0002	
IP	300.001 [b]	0.1163		0.0002	
IP	284.998 [c]	0.0399	0.0003	0.0002	
IP	286.790 [c]	0.0459	0.0002	0.0002	
IP	295.002 [c]	0.0853	0.0003	0.0002	
IP	310.001	0.2393	0.0000	0.0002	
IP	315.001	0.3293	0.0002	0.0003	
IP	319.998	0.4475	0.0002	0.0003	
IP	325.001	0.6014	0.0002	0.0003	
IP	330.001	0.7996	0.0002	0.0003	
IP	335.001	1.0522	0.0002	0.0004	
IP	340.003	1.3715	0.0002	0.0004	
IP	345.006	1.7711	0.0000	0.0005	
decane	347.447	2.0000	−0.0001	0.0001	0.040
IP	350.001	2.2664	0.0000	0.0006	
decane	353.390	2.6660	−0.0003	0.0002	0.034

TABLE 4. Continued

Method	T / K	p / kPa	Δp / kPa	σ(p) / kPa	ΔT / K
IP	354.997	2.8761	0.0000	0.0006	
IP	358.000	3.3060	−0.0001	0.0007	
decane	362.206	3.9999	0.0003	0.0003	0.025
decane	368.795	5.3330	0.0001	0.0003	0.019
decane	378.594	7.9989	−0.0003	0.0005	0.014
decane	385.943	10.6661	0.0000	0.0006	0.010
decane	391.888	13.332	0.000	0.001	0.010
decane	398.061	16.665	0.000	0.001	0.009
decane	403.190	19.933	0.000	0.001	0.008
decane	409.941	25.023	0.000	0.001	0.008
water	409.939 [a]	25.023	0.002	0.001	0.008
water	416.736	31.177	0.002	0.002	0.007
water	423.577	38.565	0.000	0.002	0.007
water	430.460	47.375	0.000	0.002	0.007
water	437.388	57.817	0.000	0.003	0.004
water	444.362	70.120	−0.002	0.003	0.004
water	451.380	84.533	−0.002	0.004	0.005
water	458.441	101.325	−0.001	0.004	0.006
water	465.546	120.790	0.006	0.005	0.006
water	472.700	143.250	0.006	0.006	0.006
water	479.894	169.02	0.01	0.01	0.005
water	487.137	198.49	0.00	0.01	0.002
water	494.419	232.02	0.01	0.01	0.005
water	501.748	270.02	−0.02	0.01	0.004

[a] The value at this temperature was not included in the fit.
[b] cr(l) phase.
[c] Supercooled liquid.

TABLE 5. Cox equation parameters

	Benzothiazole	Benzoxazole
T_{ref}/K	771	695
p_{ref}/kPa	4500	4500
A	2.47890	2.49081
10^3B	−1.72740	−1.93337
10^6C	1.50649	1.85780
T/K [a]	305 to 556	285 to 502

[a] Temperature range of the vapor pressures used in the fit.

TABLE 6. Enthalpies of vaporization obtained from the Cox and Clapeyron equations

T/K	$\Delta_l^g H_m/RK$	T/K	$\Delta_l^g H_m/RK$	T/K	$\Delta_l^g H_m/RK$
		Benzothiazole			
280.00 [a]	7386±5	380.00	6582±1	500.00	5661±19
298.15 [a]	7234±4	400.00	6430±2	520.00	5497±25
300.00 [a]	7219±4	420.00	6279±4	540.00	5327±32
320.00	7055±2	440.00	6127±6	560.00 [a]	5150±41
340.00	6894±2	460.00	5975±9	580.00 [a]	4964±51
360.00	6736±1	480.00	5820±13	600.00 [a]	4769±61
		Benzoxazole			
280.00 [a]	6490±2	400.00	5543±6	540.00 [a]	4330±55
298.15	6340±1	420.00	5387±9	560.00 [a]	4118±67
300.00	6325±1	440.00	5228±14	580.00 [a]	3889±81
320.00	6164±1	460.00	5064±19	600.00 [a]	3638±96
340.00	6006±1	480.00	4894±26	620.00 [a]	3357±112
360.00	5851±2	500.00	4716±35	640.00 [a]	3036±131
380.00	5697±4	520.00 [a]	4529±44	650.00 [a]	2855±141

[a] Values at this temperature were calculated with extrapolated vapor pressures determined from the fitted Cox coefficients.

TABLE 7. Melting-study summaries: F is the fraction melted at observed temperature T(F); T_{tp} is the triple-point temperature; x is the mole-fraction impurity

F	T(F)/K	F	T(F)/K
Benzothiazole		**Benzoxazole**	
0.168	275.623	0.154	302.396
0.320	275.636	0.303	302.449
0.522	275.642	0.453	302.468
0.674	275.645	0.602	302.477
0.826	275.646	0.801	302.484
T_{tp} = 275.651 K		T_{tp} = 302.505 K	
x = 0.00010		x = 0.00037	

TABLE 8. Molar enthalpy measurements (R=8.31451 $J \cdot K^{-1} \cdot mol^{-1}$)

N [a]	h [b]	T_i / K	T_f / K	T_{trs} / K	$\Delta_{tot}U_m$ [c] / R·K	$\Delta_{trs}H_m$ [d] / R·K	
			Benzothiazole				
			Single-phase measurements in cr(II)				
2	1	79.982	165.511		689.79	0.2	
2	1	165.524	225.168		694.86	0.3	
10	1	88.430	175.445		738.63	−0.1	
10	1	175.454	234.982		725.02	−0.0	
13	1	61.494	156.177		702.66	0.0	
13	1	156.182	202.028		494.07	−0.1	
13	1	202.048	236.466		445.37	−0.3	
			cr(II) to cr(I)				
8	2	238.194	248.265	245.0	148.26	1.9	e
9	1	238.051	247.755		144.21	3.6	e
13	1	236.464	248.118		172.80	4.5	
14	1	238.789	248.636		142.50	−1.2	e
					Average:	4.5	
			Single-phase measurements in cr(I)				
14	1	248.663	269.293		332.20	0.2	
			cr(I) to liquid				
4	6	268.422	279.749	275.651	1728.42	1514.4	
5	2	268.120	279.515		1728.16	1514.3	
14	6	269.226	278.815		1694.16	1514.4	
					Average:	1514.4	
			Single-phase measurements in liquid				
16	1	300.599	386.966		2092.02	−0.2	

TABLE 8. Continued

N [a]	h [b]	T_i / K	T_f / K	T_{trs} / K	$\Delta_{tot}U_m$ [c] / R·K	$\Delta_{trs}H_m$ [d] / R·K
			Benzoxazole			
			Single-phase measurements in cr(II)			
5	1	150.728	214.638		648.23	−0.1
8	1	54.469	100.468		258.53	0.1
8	1	100.478	151.372		388.69	0.0
8	1	151.595	205.488		535.73	−0.1
8	1	205.498	240.463		424.39	0.0
			cr(II) to cr(I)			
4	1	241.083	253.111	247.0	165.15	2.1
8	1	240.481	253.090		172.94	2.3
					Average:	2.2
			cr(I) to liquid			
1	2	298.593	306.935	302.505	2181.98	2018.7
2	6	296.330	304.948		2177.21	2018.7
8	2	294.876	305.337		2209.89	2018.4
					Average:	2018.6
			Single-phase measurements in liquid			
11	1	311.306	404.450		2189.35	0.0
11	1	404.415	442.071		971.80	0.0

[a] Adiabatic series number.

[b] Number of heating increments.

[c] $\Delta_{tot}U_m$ is the molar energy input from the initial temperature T_i to the final temperature T_f.

[d] $\Delta_{trs}H_m$ is the net molar enthalpy of transition at the transition temperature T_{trs} or the excess enthalpy relative to the heat-capacity curve described in the text for single-phase measurements.

[e] This value was not included in the average.

TABLE 9. Experimental molar heat capacities at vapor-saturation pressure ($R = 8.31451\ J \cdot K^{-1} \cdot mol^{-1}$)

N[a]	<T>/K	ΔT/K	$C_{sat,m}$[b]/R	N[a]	<T>/K	ΔT/K	$C_{sat,m}$[b]/R
			Benzothiazole				
			cr(II)				
12	5.037	1.2448	0.024	9	67.744	6.4270	5.517
11	5.274	0.9256	0.033	9	74.585	7.2552	5.871
12	6.165	1.1483	0.045	9	82.231	8.0376	6.236
11	6.233	0.9098	0.051	9	90.708	8.9181	6.618
11	7.180	0.9851	0.075	9	99.890	9.4451	7.024
12	7.209	1.0070	0.076	9	110.309	11.3858	7.489
11	8.149	1.1629	0.116	9	123.076	14.1488	8.057
12	8.224	1.0579	0.119	9	137.249	14.1977	8.704
12	9.283	1.0930	0.178	9	151.481	14.2679	9.372
12	10.386	1.1002	0.256	9	165.781	14.3368	10.089
12	11.534	1.1893	0.349	9	180.128	14.3578	10.813
12	12.868	1.3148	0.476	9	194.483	14.3889	11.592
12	14.273	1.4944	0.632	6	196.324	10.9125	11.688
12	15.834	1.6330	0.820	8	206.079	10.6394	12.202
12	17.558	1.8133	1.041	6	207.212	10.8523	12.278
12	19.470	2.0134	1.293	9	208.855	14.4467	12.368
12	21.567	2.1842	1.579	8	216.584	10.3453	12.796
12	23.883	2.4460	1.891	6	218.040	10.7970	12.881
12	26.488	2.7632	2.227	7	220.363	10.2497	12.998
12	29.386	3.0360	2.581	9	223.334	14.4770	13.174
12	32.588	3.3716	2.947	8	226.924	10.3191	13.375
12	36.163	3.7792	3.318	6	228.700	10.5137	13.474
12	40.136	4.1682	3.685	7	230.723	10.4612	13.592
12	44.556	4.6735	4.053	9	234.275	7.3660	13.801
12	49.202	4.6195	4.400	8	235.134	6.0663	13.843
12	54.389	5.7528	4.758	7	238.062	4.1957	14.014
9	56.888	4.6830	4.906	8	240.669	4.9491	14.361

TABLE 9. Continued

N[a]	<T>/K	ΔT/K	$C_{sat,m}$[b]/R	N[a]	<T>/K	ΔT/K	$C_{sat,m}$[b]/R
13	58.704	5.5557	5.030	13	242.291	11.6541	14.828
9	61.880	5.3009	5.221	9	242.903	9.7044	14.861
			cr(I)				
8	245.688	5.1539	15.068	14	258.978	20.6303	16.103
9	251.551	7.2487	15.534	8	259.409	8.1052	16.115
8	251.822	7.2370	15.576	5	263.253	10.0224	16.403
3	255.997	7.4657	15.868	3	263.435	7.4823	16.442
4	257.721	7.4287	16.007	4	265.014	7.2858	16.527
			liquid				
14	282.219	6.8483	22.289	15	370.794	14.8746	25.102
5	283.634	8.2482	22.329	15	385.608	14.7042	25.590
1	285.287	8.2372	22.376	16	396.196	18.4237	25.927
1	293.965	9.1164	22.630	15	400.249	14.5462	26.061
15	301.819	9.8302	22.878	15	414.730	14.3932	26.531
15	313.558	13.6304	23.251	16	415.407	19.9842	26.549
15	327.598	14.4364	23.693	15	429.502	15.1326	27.008
15	341.956	14.2681	24.158	16	430.785	10.7793	27.052
15	356.145	14.1067	24.622	15	441.039	7.9434	27.395
			Benzoxazole				
			cr(II)				
7	6.002	1.0164	0.049	6	66.996	6.4778	5.167
7	6.969	0.9859	0.076	6	73.814	7.1425	5.490
7	7.967	1.0374	0.118	6	81.422	7.9229	5.827
7	9.031	1.0852	0.166	4	86.487	7.6159	6.041
7	10.096	1.0674	0.231	4	94.980	9.3577	6.391
7	11.226	1.1961	0.311	4	104.523	9.7017	6.770
7	12.479	1.2920	0.408	4	114.379	9.9964	7.167
7	13.830	1.4060	0.527	4	124.405	10.0437	7.568
7	15.307	1.5479	0.676	4	134.577	10.1467	7.984

TABLE 9. Continued

N[a]	<T>/K	ΔT/K	$C_{sat,m}$[b]/R	N[a]	<T>/K	ΔT/K	$C_{sat,m}$[b]/R
7	16.947	1.7333	0.852	4	144.658	10.0048	8.407
7	18.781	1.9327	1.060	4	154.651	9.9675	8.828
7	20.823	2.1563	1.304	4	164.717	10.1500	9.288
7	23.123	2.4369	1.589	4	174.876	10.1541	9.755
7	25.686	2.6902	1.902	4	185.092	10.2667	10.246
7	28.546	3.0289	2.242	4	195.428	10.2787	10.740
7	31.738	3.3538	2.603	4	205.636	10.1257	11.249
7	35.270	3.7148	2.973	4	215.637	9.8667	11.758
7	39.181	4.1051	3.342	5	219.826	10.3640	11.973
7	43.507	4.5465	3.708	4	225.685	10.2115	12.280
7	48.292	5.0222	4.066	5	230.078	10.1001	12.511
7	53.613	5.6181	4.429	4	235.917	10.2429	12.818
6	55.298	5.0669	4.520	5	238.102	5.9432	12.940
6	60.794	5.9074	4.844				
			cr(l)				
3	254.740	6.8809	14.197	8	284.748	20.3283	16.307
4	257.209	8.0024	14.337	1	289.730	5.9361	16.648
8	268.766	11.8901	15.138	2	290.513	11.6865	16.776
1	283.847	5.8445	16.169	1	295.645	5.9215	17.620
			liquid				
8	308.926	7.1796	21.822	9	348.806	15.0269	23.181
2	309.429	8.9684	21.845	9	364.189	15.7421	23.722
9	310.573	9.7327	21.878	10	380.978	19.1561	24.313
1	311.409	8.9513	21.912	10	400.407	19.7288	25.001
1	320.509	9.2542	22.210	10	420.388	20.2790	25.708
9	321.226	11.5634	22.228	10	437.422	13.8601	26.307
9	334.152	14.2802	22.672				

a Adiabatic series number.

b Average heat capacity for a temperature increment of ΔT with a mean temperature <T>.

TABLE 10. Molar thermodynamic functions at vapor-saturation pressure [a]
($R = 8.31451\ J \cdot K^{-1} \cdot mol^{-1}$)

$\frac{T}{K}$	$\frac{C_{sat,m}}{R}$	$\frac{\Delta_0^T S_m}{R}$	$\frac{\Delta_0^T H_m}{RT}$	$\frac{T}{K}$	$\frac{C_{sat,m}}{R}$	$\frac{\Delta_0^T S_m}{R}$	$\frac{\Delta_0^T H_m}{RT}$
			Benzothiazole				
			cr(II)				
5.000	0.025	0.008	0.006	110.000	7.475	7.804	4.234
10.000	0.227	0.070	0.053	120.000	7.920	8.473	4.523
15.000	0.718	0.246	0.186	130.000	8.371	9.125	4.801
20.000	1.365	0.540	0.398	140.000	8.830	9.762	5.073
25.000	2.037	0.917	0.659	150.000	9.302	10.387	5.339
30.000	2.653	1.344	0.941	160.000	9.796	11.003	5.602
35.000	3.202	1.795	1.226	170.000	10.299	11.612	5.863
40.000	3.673	2.254	1.503	180.000	10.809	12.215	6.124
45.000	4.087	2.711	1.768	190.000	11.343	12.814	6.384
50.000	4.460	3.162	2.019	200.000	11.886	13.409	6.646
60.000	5.101	4.033	2.481	210.000	12.433	14.002	6.908
70.000	5.644	4.861	2.895	220.000	12.987	14.593	7.172
80.000	6.131	5.647	3.269	230.000	13.550	15.183	7.437
90.000	6.586	6.396	3.613	240.000	14.128	15.772	7.704
100.000	7.029	7.113	3.932	245.000 [b]	14.428	16.066	7.838
			cr(I)				
245.000 [b]	15.048	16.085	7.856	270.000 [b]	16.897	17.636	8.609
250.000	15.427	16.393	8.004	275.651 [b]	17.298	17.990	8.783
260.000	16.171	17.012	8.304				
			liquid				
275.651 [b]	22.094	23.484	14.277	420.000	26.700	33.68	17.744
280.000	22.223	23.831	14.399	440.000	27.361	34.93	18.166
290.000	22.512	24.616	14.674	460.00	28.09	36.17	18.58
298.150	22.761	25.243	14.891	480.00	28.80	37.38	18.99
300.000	22.820	25.384	14.940	500.00	29.50	38.57	19.40
320.000	23.454	26.877	15.452	520.00	30.19	39.74	19.80
340.000	24.094	28.318	15.942	540.00	30.81	40.89	20.20

TABLE 10. continued

T/K	$C_{sat,m}/R$	$\Delta_0^T S_m/R$	$\Delta_0^T H_m/RT$	T/K	$C_{sat,m}/R$	$\Delta_0^T S_m/R$	$\Delta_0^T H_m/RT$
360.000	24.748	29.714	16.413	560.00	31.48	42.02	20.59
380.000	25.406	31.070	16.869	580.00	32.01	43.14	20.97
400.000	26.053	32.389	17.312	600.00	32.60	44.23	21.35

Benzoxazole

cr(II)

5.000	0.028	0.009	0.007	110.000	6.990	7.266	3.960
10.000	0.225	0.076	0.057	120.000	7.391	7.891	4.229
15.000	0.644	0.239	0.177	130.000	7.796	8.499	4.488
20.000	1.205	0.499	0.362	140.000	8.210	9.091	4.739
25.000	1.819	0.834	0.592	150.000	8.629	9.672	4.984
30.000	2.409	1.218	0.846	160.000	9.070	10.243	5.226
35.000	2.946	1.631	1.109	170.000	9.530	10.807	5.465
40.000	3.414	2.056	1.368	180.000	10.000	11.364	5.704
45.000	3.824	2.482	1.619	190.000	10.479	11.918	5.943
50.000	4.192	2.904	1.858	200.000	10.965	12.468	6.182
60.000	4.795	3.723	2.299	210.000	11.466	13.015	6.421
70.000	5.313	4.503	2.694	220 000	11.979	13.560	6.662
80.000	5.765	5.242	3.050	230.000	12.497	14.104	6.905
90.000	6.187	5.946	3.375	240.000	13.034	14.647	7.149
100.000	6.591	6.619	3.677	247.000 [b]	13.406	15.027	7.321

cr(I)

247.000 [b]	13.660	15.036	7.329	290.000	16.497	17.450	8.479
250.000 [b]	13.860	15.202	7.407	298.150	17.029	17.915	8.706
260.000	14.523	15.758	7.668	300.000 [b]	17.149	18.021	8.757
270.000	15.184	16.319	7.934	302.505 [b]	17.312	18.164	8.827
280.000	15.842	16.883	8.204				

liquid

280.000 [b]	20.880	23.195	15.039	440.000	26.394	33.765	18.150
290.000 [b]	21.203	23.933	15.246	460.00	27.11	34.95	18.52

TABLE 10. continued

$\frac{T}{K}$	$\frac{C_{sat,m}}{R}$	$\frac{\Delta_0^T S_m}{R}$	$\frac{\Delta_0^T H_m}{RT}$	$\frac{T}{K}$	$\frac{C_{sat,m}}{R}$	$\frac{\Delta_0^T S_m}{R}$	$\frac{\Delta_0^T H_m}{RT}$
298.150 [b]	21.469	24.525	15.412	480.00	27.89	36.12	18.90
300.000 [b]	21.530	24.658	15.450	500.00	28.61	37.28	19.27
302.505 [b]	21.612	24.837	15.500	520.00	29.39	38.41	19.65
310.000	21.860	25.369	15.651	540.00	30.10	39.54	20.02
320.000	22.186	26.068	15.850	560.00	30.81	40.64	20.39
340.000	22.875	27.434	16.243	580.00	31.58	41.74	20.76
360.000	23.574	28.761	16.631	600.00	32.32	42.82	21.14
380.000	24.279	30.054	17.015	620.00	33.29	43.90	21.51
400.000	24.987	31.318	17.396	640.00	34.49	44.97	21.90
420.000	25.694	32.554	17.774	650.00	35.25	45.51	22.10

[a] Values listed in this table are reported with one digit more than is justified by the experimental uncertainty. This is to avoid round-off errors in the calculation of values listed in table 15.

[b] Values at this temperature were calculated with graphically extrapolated heat capacities.

TABLE 11. Experimental $C^{II}_{x,m}/R$ values ($R = 8.31451\ J \cdot K^{-1} \cdot mol^{-1}$)

mass/g	0.015946	0.010353	0.028303	0.020138	0.010034	0.014802
Vol. cell/cm^3 [a]	0.05440	0.05470	0.05409	0.05288	0.05288	0.05292
T/K	$C^{II}_{x,m}/R$	$C^{II}_{x,m}/R$	$C^{II}_{x,m}/R$	$C^{II}_{x,m}/R$	$C^{II}_{x,m}/R$	$C^{II}_{x,m}/R$
	Benzothiazole			**Benzoxazole**		
315.0	23.5	23.1	23.3	22.0	21.8	21.9
335.0	24.0	23.7	23.9	22.8	22.7	22.6
355.0	24.6	24.2	24.6	23.6	23.3	23.3
375.0	25.2	25.0	25.2	24.3	24.3	24.1
395.0	25.9	25.6	25.9	25.0	25.1	24.8
415.0	26.7	26.5	26.6	25.9	25.6	25.6
435.0	27.4	27.3	27.3	26.5	27.5	26.7
455.0	28.1	28.2	28.0	27.5	28.3	27.4
475.0	29.0	29.1	28.7	28.4	29.8	28.8
495.0	29.8	30.3	29.4	29.3	30.9	29.6
515.0	30.7	31.5	30.1	30.2	32.0	30.7
535.0	31.4	32.2	30.8	31.1	33.5	31.7
555.0	33.4	35.5	31.6	32.2	34.6	32.8
575.0	32.8	35.5	32.6	33.1	36.6	33.7
595.0	34.5	35.6	33.0	34.0	38.2	35.3
615.0				35.5	41.1	35.9
635.0				36.6	42.6	37.4
655.0				38.8	43.6	40.1

[a] Volume measured at 298.15 K.

TABLE 12. Parameters for equations (**13**) and (**14**), estimated critical constants and acentric factor for benzoxazole [a]

Benzoxazole			
A	2.49488	b_0	−0.32822
B	−1.35611	b_1	−0.74389
C	0.90679	b_2	1.36926
		b_3	−1.56416

T_c = 695 K p_c = 4500 kPa ρ_c = 349 kg·m^{-3} ω = 0.362

[a] Values for the critical constants and acentric factor are estimates derived from the fitting procedures (see text).

TABLE 13. Values of $C^{II}_{v,m}(\rho = \rho_{sat})/R$ and $C_{sat,m}/R$ ($R = 8.31451\ J \cdot K^{-1} \cdot mol^{-1}$)

T/K	$C^{II}_{v,m}(\rho = \rho_{sat})/R$	$C_{sat,m}/R$	T/K	$C^{II}_{v,m}(\rho = \rho_{sat})/R$	$C_{sat,m}/R$
		Benzothiazole			
320.0	23.5	23.5	480.0	28.8	28.8
340.0	24.1	24.1	500.0	29.5	29.5
360.0	24.7	24.7	520.0	30.1	30.2
380.0	25.4	25.4	540.0	30.8	30.8
400.0	26.0	26.0	560.0	31.4	31.5
420.0	26.7	26.7	580.0	31.9	32.0
440.0	27.4	27.4	600.0	32.4	32.6
460.0	28.1	28.1			
		Benzoxazole			
320.0	22.2	22.2	500.0	28.6	28.6
340.0	22.9	22.9	520.0	29.3	29.4
360.0	23.6	23.6	540.0	29.9	30.1
380.0	24.3	24.3	560.0	30.6	30.8
400.0	25.0	25.0	580.0	31.2	31.6
420.0	25.7	25.7	600.0	31.8	32.3
440.0	26.4	26.4	620.0	32.5	33.3
460.0	27.1	27.1	640.0	33.1	34.5
480.0	27.8	27.9	660.0	34.0	36.5

TABLE 14. Thermodynamic properties in the ideal-gas state
(R = 8.31451 $J \cdot K^{-1} \cdot mol^{-1}$ and p° = 101.325 kPa)

T / K	$\frac{\Delta_0^T H_m^\circ}{RT}$	$\frac{\Delta_{imp} H_m^\circ}{RT}$ [a]	$\frac{\Delta_0^T S_m^\circ}{R}$	$\frac{\Delta_{imp} S_m^\circ}{R}$ [b]	$\frac{\Delta_f H_m^\circ}{RT}$	$\frac{\Delta_f S_m^\circ}{R}$	$\frac{\Delta_f G_m^\circ}{RT}$
Benzothiazole							
280.00 [c]	40.78±0.02	0.00	39.49±0.03	0.00	58.72±0.16	−28.62±0.03	87.35±0.16
298.15 [c]	39.15±0.02	0.00	40.38±0.03	0.00	54.84±0.15	−28.95±0.03	83.78±0.16
300.00 [c]	39.00±0.02	0.00	40.47±0.03	0.00	54.47±0.15	−28.98±0.03	83.45±0.15
320.00	37.50±0.02	0.00	41.43±0.03	0.00	50.75±0.14	−29.30±0.03	80.05±0.15
340.00	36.22±0.02	0.00	42.39±0.03	0.00	47.49±0.13	−29.59±0.03	77.07±0.14
360.00	35.13±0.02	0.01	43.34±0.03	0.00	44.59±0.13	−29.85±0.03	74.44±0.13
380.00	34.20±0.02	0.01	44.28±0.03	0.01	42.02±0.12	−30.08±0.03	72.10±0.12
400.00	33.40±0.02	0.02	45.21±0.03	0.01	39.72±0.11	−30.28±0.03	70.01±0.12
420.00	32.72±0.02	0.03	46.14±0.03	0.02	37.65±0.11	−30.46±0.03	68.12±0.11
440.00	32.13±0.02	0.04	47.07±0.04	0.03	35.78±0.11	−30.63±0.04	66.41±0.11
460.00	31.63±0.03	0.06	47.98±0.04	0.05	34.09±0.10	−30.77±0.04	64.86±0.11
480.00	31.21±0.04	0.09	48.89±0.05	0.07	32.55±0.10	−30.89±0.05	63.44±0.11
500.00	30.84±0.05	0.12	49.80±0.06	0.09	31.14±0.11	−31.00±0.06	62.14±0.11
520.00	30.54±0.07	0.16	50.70±0.08	0.12	29.85±0.11	−31.09±0.08	60.94±0.12
540.00	30.28±0.08	0.22	51.59±0.09	0.16	28.67±0.12	−31.17±0.09	59.84±0.12
560.00 [c]	30.06±0.10	0.28	52.47±0.11	0.20	27.58±0.13	−31.23±0.11	58.81±0.13
580.00 [c]	29.88±0.12	0.35	53.35±0.13	0.26	26.57±0.14	−31.28±0.13	57.86±0.14
600.00 [c]	29.73±0.14	0.43	54.21±0.15	0.32	25.64±0.16	−31.32±0.15	56.96±0.15
Benzoxazole							
280.00 [c,d]	38.22±0.02	0.00	38.12±0.02	0.00	19.79±0.23	−28.62±0.02	48.41±0.23
298.15 [d]	36.68±0.02	0.00	38.94±0.02	0.00	18.21±0.21	−29.00±0.02	47.22±0.21
300.00 [d]	36.53±0.02	0.00	39.02±0.02	0.00	18.07±0.21	−29.04±0.02	47.11±0.21
320.00	35.12±0.02	0.00	39.91±0.03	0.00	16.57±0.20	−29.42±0.03	45.99±0.20
340.00	33.92±0.02	0.01	40.80±0.03	0.01	15.26±0.19	−29.76±0.03	45.03±0.19
360.00	32.90±0.02	0.02	41.69±0.03	0.01	14.12±0.18	−30.06±0.03	44.19±0.18
380.00	32.03±0.02	0.03	42.58±0.03	0.02	13.11±0.17	−30.34±0.03	43.45±0.17
400.00	31.30±0.02	0.04	43.47±0.03	0.03	12.22±0.16	−30.58±0.03	42.80±0.16
420.00	30.67±0.03	0.07	44.36±0.04	0.05	11.43±0.15	−30.79±0.04	42.22±0.15

TABLE 14. continued

T / K	$\frac{\Delta_0^T H_m^\circ}{R\,T}$	$\frac{\Delta_{imp} H_m^\circ}{R\,T}$ [a]	$\frac{\Delta_0^T S_m^\circ}{R}$	$\frac{\Delta_{imp} S_m^\circ}{R}$ [b]	$\frac{\Delta_f H_m^\circ}{R\,T}$	$\frac{\Delta_f S_m^\circ}{R}$	$\frac{\Delta_f G_m^\circ}{R\,T}$
440.00	30.13±0.04	0.10	45.23±0.05	0.07	10.72±0.15	−30.99±0.05	41.71±0.15
460.00	29.67±0.05	0.14	46.11±0.06	0.10	10.08±0.14	−31.16±0.06	41.24±0.14
480.00	29.29±0.06	0.19	46.98±0.07	0.14	9.51±0.15	−31.32±0.07	40.83±0.14
500.00	28.96±0.08	0.26	47.84±0.09	0.19	8.99±0.15	−31.45±0.09	40.44±0.14
520.00 [c]	28.69±0.10	0.34	48.71±0.11	0.25	8.53±0.16	−31.57±0.11	40.10±0.14
540.00 [c]	28.47±0.12	0.43	49.57±0.13	0.31	8.11±0.17	−31.67±0.13	39.78±0.15
560.00 [c]	28.28±0.15	0.53	50.42±0.15	0.39	7.73±0.18	−31.75±0.15	39.48±0.15
580.00 [c]	28.12±0.17	0.65	51.26±0.17	0.48	7.38±0.20	−31.83±0.17	39.20±0.16
600.00 [c]	27.99±0.20	0.79	52.10±0.20	0.59	7.05±0.22	−31.90±0.20	38.95±0.17
620.00 [c]	27.88±0.22	0.95	52.91±0.22	0.71	6.74±0.24	−31.96±0.22	38.70±0.19
640.00 [c]	27.77±0.25	1.12	53.71±0.25	0.84	6.44±0.27	−32.03±0.25	38.47±0.20
650.00 [c]	27.71±0.27	1.22	54.09±0.27	0.92	6.29±0.28	−32.07±0.27	38.36±0.21

a Gas-imperfection correction included in the ideal-gas enthalpy.

b Gas-imperfection correction included in the ideal-gas entropy.

c Values at this temperature were calculated with extrapolated vapor pressures calculated from the fitted Cox coefficients.

d Values at this temperature were calculated with extrapolated liquid-phase heat capacities.

TABLE 15. Comparison of benzoxazole vapor pressures below the triple-point temperature

T / K	p{cr(l)} [a] / Pa	p(liquid) [b] / Pa	p(calc) [c] / Pa	Δ(p) [d] / Pa
280.003	16.5	26.5	15.7	0.8
284.999	27.5	39.7	26.5	1.0
290.001	45.0	58.5	44.1	0.9
295.001	72.8	85.0	71.9	0.9
300.001	116.3	121.7	115.2	1.1

[a] Sublimation pressure measured in inclined piston.

[b] Vapor pressure for supercooled liquid calculated using the Cox equation parameters listed in table 5.

[c] Sublimation pressure calculated using equation (19).

[d] p{cr(l)} – p(calc) deviation between measured and calculated values of the sublimation pressure.

END

DATE FILMED

10 / 29 / 91